



**HAL**  
open science

# Toward Radio Access Network Slicing Enforcement in Multi-Cell 5G System

Imane Oussakel, Philippe Owezarski, Pascal Berthou, Laurent Houssin

► **To cite this version:**

Imane Oussakel, Philippe Owezarski, Pascal Berthou, Laurent Houssin. Toward Radio Access Network Slicing Enforcement in Multi-Cell 5G System. *Journal of Network and Systems Management*, 2023, 31, pp.8. 10.1007/s10922-022-09694-0 . hal-02633510v2

**HAL Id: hal-02633510**

**<https://hal.science/hal-02633510v2>**

Submitted on 20 Oct 2022

**HAL** is a multi-disciplinary open access archive for the deposit and dissemination of scientific research documents, whether they are published or not. The documents may come from teaching and research institutions in France or abroad, or from public or private research centers.

L'archive ouverte pluridisciplinaire **HAL**, est destinée au dépôt et à la diffusion de documents scientifiques de niveau recherche, publiés ou non, émanant des établissements d'enseignement et de recherche français ou étrangers, des laboratoires publics ou privés.

# Toward Radio Access Network Slicing Enforcement in Multi-Cell 5G System

Imane Oussakel<sup>1</sup>, Philippe Owezarski<sup>1\*</sup>, Pascal Berthou<sup>1</sup>  
and Laurent Houssin<sup>1,2</sup>

<sup>1</sup>LAAS-CNRS, Université de Toulouse, CNRS, Toulouse, 31400,  
France.

<sup>2</sup>ISAE-SUPAERO, Université de Toulouse, Toulouse, 31400,  
France.

\*Corresponding author(s). E-mail(s): [philippe.owezarski@laas.fr](mailto:philippe.owezarski@laas.fr);  
Contributing authors: [imane.oussakel@laas.fr](mailto:imane.oussakel@laas.fr);  
[pascal.berthou@laas.fr](mailto:pascal.berthou@laas.fr); [laurent.houssin@isae-superaero.fr](mailto:laurent.houssin@isae-superaero.fr);

## Abstract

The proliferation of sophisticated applications and services comes with diverse performance requirements. The 5G cellular network is advocated to support this diversity through an end-to-end network slicing. Even-though the slicing is not a novel concept, its implementation in the RAN still remains challenging. In this article, we aim to enforce the real time 5G slicing from radio resources perspective in a multi-cell system. For that, an exact optimization model is proposed. Due its high convergence time, heuristics are developed and evaluated with regard to the optimal model. Results are promising, as two heuristics are highly enforcing the real time RAN slicing.

**Keywords:** Radio Access Network (RAN), RAN Slicing, 5G, Optimization, Resource allocation.

## 1 Introduction

The tremendous growth of services and applications demand is increasing over the years with diverse Quality of Service (QoS), for example for real-time, streaming, or control applications to quote a few. 3GPP and other

organizations aim to support this variety of services requirements through 5G system with a service-based architecture. Three families of services have been standardized : enhanced Mobile BroadBand (eMBB), ultra Reliable Low Latence Communications (uRRLC), and massive Machine Type Communications (mMTC). These services are classically devoted to high speed multimedia communication for residential users, system or application control, and machine-to-machine communication as in the Internet of Things (IoT).

Network slicing is considered as one of the pillars to enable such architecture where each Mobile Network Operator (MNO) shares its physical infrastructure with several tenants of slices. The fulfillment of the envisioned network slicing approach involves high flexibility and programmability of 5G network. Chahbar et al. [1] and Shen et al. [2] provide a synthetic view of the network slicing in the 3GPP framework. To that end, virtualization and softwarization based solutions have been nominated, mainly Network Function Virtualization (NFV)[3] and Software Defined Network (SDN) [4] based solutions. The former allows flexibility of Network Functions (NFs) via virtualization, and the latter separates the control from the user data functions with a centralized controller. Several prototypes based on NFV and SDN have been proposed to address the Core Network (CN) [5] and Radio Access Networks (RAN) [6, 7] slicing. The SDN implementation at the RAN part is referred by Software Defined RAN (SD-RAN).

The enforcement of RAN slicing still attracts the academy and industries researchers attention, as maintaining slices isolation with efficient use of radio resources is a challenging task. In fact, because of the scarcity of radio resources, the resources over-provisioning principle used in the CN cannot be extended to RAN. Hence, the wireless resource allocation needs to meet the service requirements for each slice regardless the channel conditions or network congestion, while efficiently using the scarce available resources. Moreover, the 5G system framework is subdivided into three layers, infrastructure, network and service layers. Isolation must be sustained over the different system layers. Particularly, the outage performance of one slice, i.e. congestion, attack or QoS degradation, should not impact negatively the other available slices in the network.

The enforcement of RAN slicing is based on the slice performance requirements, the traffic demand and the channel/network conditions, the amount of the slice required resources should be decided. This is known by resource slicing policy. The implementation of such policy (i.e. dynamic resources allocation) has to respect the RAN slicing requirements formulated and summarized as follows:

- Orthogonality (resource isolation): it must be guaranteed between slices. Each radio resource in terms of time and frequency, must be allocated to only one slice to avoid inter-slices interference, thus ensuring the slice isolation at the radio resources level.
- Satisfaction: each slice has to be allocated the amount of assigned resources based on the slicing policy, i.e. for a given slice that has been

assigned 25 radio resources, it should receive approximately the amount of 25 radio resources, without excess. This way the slice demand is satisfied and each slice fully uses its resources.

- Scalability: the MNO should be able to scale up/down the slice allocated resources with respect to the network conditions and slice demand variation. Moreover, as the slices are created dynamically and on-demand, the radio resource model should allow the MNO to serve new slice requests. This can be achieved through the reuse of the unallocated resources during the allocation window.
- Cooperation enabling: the 5G advanced radio techniques such as IBSPC (inter-base station power control) and CoMP (coordinated multi-point) that mitigate interference involve a tight cooperation between the base stations (i.e. gNBs in case of 5G) to achieve their objective [8]. As the RAN slicing imposes the slices resources orthogonality, the activation of the appropriate technology is based on the slice performance requirements and SLA. The slices radio resources allocation should therefore ease the deployment of these advanced technologies for each tenant.

The achievement of these requirements is considered as a RAN slicing enforcement problem. In this article we focus on its resolution in the context of 5G system at radio resources level as it still remains under-explored. For that, RAN resources allocation strategies are proposed as to achieve the aforementioned RAN slicing enforcement requirements. This slice resources allocation problem deals with autonomously and continuously optimizing radio resources placement at run-time. Given the constraints to be respected throughout this allocation process, constraint programming is the ideal optimization technique. In this work, the RAN slicing enforcement problem is then modeled as a set of objectives to achieve, and constraints to be respected. This model is then entered in an optimization solver in order to provide at any time, depending on user services requests, the optimal allocation of available radio resources to slices. The problem with the solver deals with the significantly large amount of time it can take to provide the optimal resources allocation to slices: as the problem to be solved is NP-hard, the optimization process converges slowly. As we need to run this resource allocation problem in real-time, it is then needed to design some heuristics able to provide an optimal (or near-optimal) result in real-time. Three heuristics are proposed in this paper. They are validated by demonstrating that they statistically nearly reach the same optimal allocation obtained by the solver with the exact model, in very short time.

Further, the rest of this paper is organized as follows. The RAN slicing enforcement problem is introduced in section 2 with an explanation of the 5G radio novelty. The related work is reviewed in section 3. Section 4 exhibits the system design and the proposed model. The developed model is shown to converge slowly as evaluated in section 5. It then limits the RAN slicing enforcement for real time scenarios. Therefore, we propose in Section 6 three heuristics that enforce the real time slicing. Then, a comparison of the three

algorithms performance with respect to the optimal values given by the mathematical model is conducted in section 7. Finally, section 8 concludes this paper with open issues and future work.

## 2 RAN slicing enforcement problem

This section covers the important 5G terminologies required for the exhibition of the RAN slicing problem. Mainly, the 5G radio resources structure is presented. Then, the RAN slicing enforcement problem is explained and the required allocations strategies to achieve the above-mentioned requirements are highlighted.

### 2.1 5G background

In 5G system, the physical layer is more flexible with respect to the previous generations. Radio resources in 4G are uniformly distributed over a time-frequency grid that is decomposed into resource blocks (RB) of 1 ms over 12 sub-carriers spaced by 15 kHz. In order to fulfill the variety of services requirements, increase the network reliability and adapt to frequency range, 5G introduces different radio frames numerologies for lower frequency bands (i.e. sub-6 GHz), and higher frequency bands such as millimeter waves (i.e. above-6 GHz).

Table 1 exhibits the different numerologies standardized by 3GPP. They are separated based on the frequency band (i.e. sub-6 GHz and above-6 GHz bands). Each given numerology  $\mu$ <sup>1</sup> defines the time-frequency resource size in one Transmission Time interval (TTI), TTI=1ms. A numerology  $\mu$  refers to the sub-carrier spacing (SCS) in frequency domain and the slot duration in time domain. For instance, as depicted in Fig. 1, for  $\mu = 1$ , the radio resource size is fixed to 0.5 ms over 12 sub-carriers spaced by 30 KHz. In general, the SCS scales by  $2^\mu * 15kHz$  and the slot duration decreases with higher numerology ( $\mu$ ). Such flexibility is essentially introduced as to achieve the diverse services requirements. For example, it is preferable to transmit latency sensitive services in shorter time interval with larger sub-carrier spacing, e.g.  $\mu = 4$ . Due to the limited spectrum in lower frequency bands, only numerologies 0, 1 and 2 are authorized to be used in the sub-6GHz. On the other hand, numerologies 3 and 4 have to be used for higher frequency bands (above-6 GHz). As the main difference between the numerologies of sub-6 GHz and above-6 GHz is the SCS and slot duration, we chose to illustrate this article with examples from the sub-6 GHz bands. The same developed approaches can be applied for bands above-6 GHz by only modifying the numerology types, i.e. considering numerologies 3 and 4.

In order to support the coexistence of the multiple numerologies on same carrier, the resources are structured in the so-called tiles [9]. The tile is the smallest subset of frequency and time resources allocated to a particular

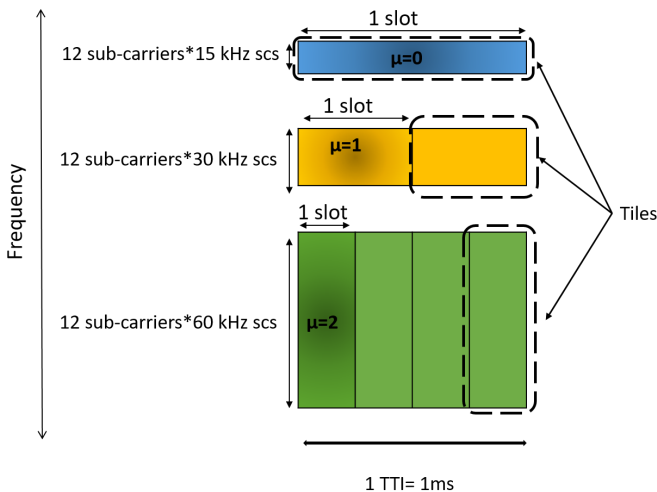
---

<sup>1</sup>3GPP, TR 38.802, TR 38.804: Study on new radio access technology Physical layer aspects, Study on new radio access technology Radio interface protocol aspects. <https://www.3gpp.org/>

**Table 1:** 5G Standard radio frames numerologies subdivided into sub-6 GHz and above-6 GHz bands

Frequency band	$\mu$	SCS (kHz)	Slot duration (ms)
Sub-6 Ghz	0	15	1
	1	30	0.5
	2	60	0.25
Above- 6 Ghz	3	120	0.125
	4	240	0.0625

slice/service with same numerology  $\mu$ . Hence, for sub-6 GHz, three tile structures are tailored as shown in Fig. 1. For instance, the tile structure for  $\mu = 0$  is 1 ms over 12 subcarriers spaced by 15 KHz. Further, multiplexing over time and frequency is required for the transmission of the different numerologies, e.g. over time, 3GPP imposes symbol alignment between tiles to ensure orthogonality.

**Fig. 1:** Sub-6 GHz numerologies

## 2.2 Problem Formulation

The enforcement of 5G RAN slicing approach rises many requirements, as indicated in section 1, mainly scalability, orthogonality, slices satisfaction and easing the inter-base stations cooperation. In the following, resources refer to the radio resources.

To tackle the scalability requirement, the RAN should be more flexible about the radio resources allocation. The RAN slicing enforcement algorithms

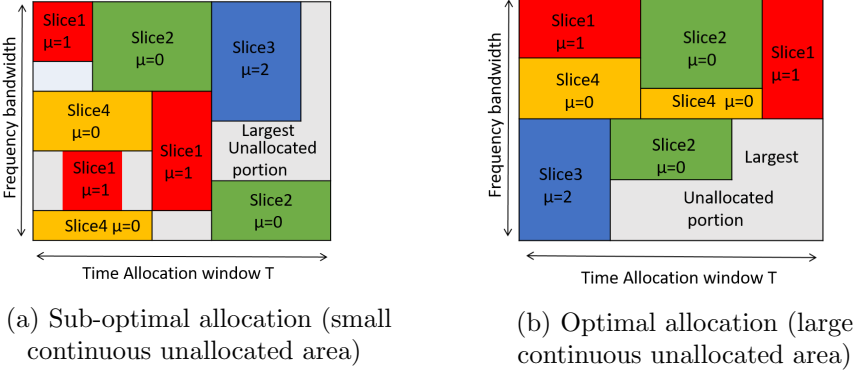


**Fig. 2:** Optimal and sub-optimal resource allocation

should then allocate resources in a way that maximizes the adjacency of the unallocated portion of resources, instead of having sparse unallocated resources in the time-frequency grid. This objective is illustrated in Fig. 2. Two time-frequency resource grids are schematized as to explain the difference between an optimal (b) and sub-optimal (a) resource allocation for 4 slice requests in 5G context. Each of the 4 slices demands a different amount of resources with specific numerology, i.e. a number of tiles. Even-though both allocations (a) and (b) satisfy the four slice requests during the allocation window  $T$ , it is clear that the allocation strategy in (a) is sub-optimal compared to (b). In fact, the resource allocation strategies as in (a) might lead to inefficient resource utilization as they do not consider the different tile structures during the allocation process. 5G proposes a variety of tile structures, and some allocation strategies induce a small sparse unallocated resources over the resource grid, as represented in Fig. 2 (a). Those small leaved resources are considered as wasted as they do not fit any tile structure. Only, the small continuous unallocated portion of resources is then reused by the MNO. In contrast, the allocation strategy in (b) results in a large unallocated portion of resources. Hence, it allows the MNO to further reuse the unallocated resources in an efficient manner, as different structures could fit in this portion, e.g. the sudden delay-critical requests could also be considered by the MNO. Thus, it enables the scalability requirement and increases the resource utilization efficiency.

On the other hand, in 5G context, each geographical area is covered by different cells types. Thus, high level of interference is expected. It includes the inter-slice as well as the intra-slice interference. The intra-slice interference is out of the scope of this work. To illustrate the inter-slice interference, let us consider two adjacent gNBs (BS1 and BS2), close enough to interfere. The top scheme of Fig. 3 schematizes their resources allocation for 3 slices. Each slice has a different time-frequency resources portion on each gNB. As the gNBs are adjacent and the slices deploy different techniques to manage the transmission over their resources, the inter-slice interference is induced. Particularly, an inter-slice interference is observed between slice 2 and slice 3, as slice 3 is

allocated the left lower resources portion on BS1, while the same portion on BS2 is allocated to slice 2. Such interference type is hard to manage, as each tenant monitors its resources independently from the other tenants. Moreover, 5G strategies for interference mitigation rely on a tight cooperation and coordination among the adjacent gNBs in the network, i.e. cooperation enabling requirement.

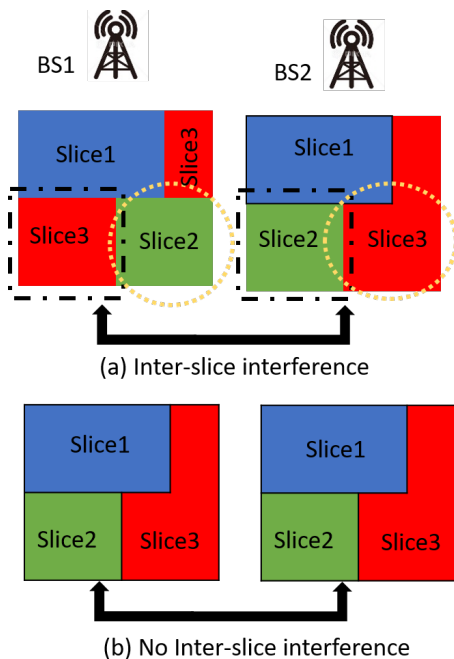


**Fig. 3:** Resource allocation for inter-slice interference mitigation

Therefore, the RAN slicing enforcement algorithms should guarantee the allocation of the same radio resources over time and frequency to the same slices among the adjacent gNBs. Such allocation eases not only the deployment of 5G advanced techniques such as MIMO and beamforming, but also the transmission schemes for inter-slice interference mitigation. Thus, it improves the overall network performance. Through experimentation, D’Oro et al [10] proved the ability of such allocation to double the network throughput compared to a random allocation.

Fig. 3 (b) depicts the idea, each slice is allocated the same time-frequency portion of resources on both gNBs. Hence, inter-slice interference is absent. Also, the slice owners have more flexibility to mitigate intra-slice interference and enable the advanced 5G techniques (e.g. beamforming, IBSPC, CoMP). Clearly the allocation strategy in (b) is optimal for the RAN slicing enforcement in 5G compared to the random allocation approach in (a), where each



gNB allocates its resources independently from the adjacent gNBs. That is, the RAN slicing enforcement requires a coordinated resources allocation over adjacent gNBs.

On the other hand, in order to achieve this optimal allocation, the complexity of resources allocation strategy increases. In fact, to enable the coordination between the adjacent gNBs, the gNBs could either communicate directly with each other or through a controller. The inconvenient of the direct communication between gNBs is the increase of signaling traffic. Thus, adding a controller (SD-RAN) is considered as the ultimate solution as would be exhibited in part 4.

Further, we argue that the combination of both allocation strategies (fig. 3 (b) and fig. 2 (b)) allows the realization of the challenging RAN slicing requirements. For that, we address the optimization of such strategy in the upcoming parts.

### 3 Related work

In the context of RAN slicing, resource management and orchestration have received significant interest from the research community. Many frameworks [6, 11–13] have been proposed to deal with the high level wireless resource orchestration and management. While the proposed approaches are effective in resource control and orchestration, they might lack effectiveness for fine grained control scenarios, where performing and enabling advanced 5G transmission techniques are required. Also, a major challenge with these frameworks is the efficient resource allocation while preserving the radio resources isolation. A data-driven approach to quantify the efficiency of resource sharing in future sliced networks [14] has confirmed that SLAs defined in terms of guaranteed time slots allow much more flexibility in balancing efficiency and QoS but should enable a fast enough re-orchestration of network resources to be useful.

Recently, researches have converged to enforce the RAN slicing from a resource allocation aspect. To overcome the static resources segmentation limitations, shared allocation strategies are proposed [15–17]. For instance, B.Han et al. [17], Yang et al. [18] propose the use of Genetic algorithm to optimize resource management between heterogeneous slices with maximized long-term network utility. Although the proposed methods gain in terms of multiplexing, they lack of programmability and resources isolation aspects, that allow each tenant to manage its resources independently. By introducing resources virtualization, Chang et al. [19] formulate the problem as a knapsack problem. An algorithm is proposed to maximize the number of accepted slices with an efficient 5G resource partitioning. Papa et al. [20] solve the problem using a Lyapunov optimisation approach. Nevertheless, all of the above-mentioned contributions consider a network with only one gNB, which limits the deployment of their approaches in a multi-gNB network, where each tenant requires a different amount of resources on each gNB, based on the channel condition

and the number of connected users. Moreover, the inter-cell interference is not addressed, i.e. cooperation enabling requirement. For instance, Ojaghi et al. [21] propose a RAN slicing mechanism that only considers isolation and satisfaction. The mechanism and model do not take into account scalability or optimization over several gNBs. The model uses the Mixed Integer Programming (MIP), and to cope with computation time, Ojaghi et al. propose a faster and near optimal heuristic (SlicedRAN). Hossain and Ansari [22] deal with the slicing issue at the frequency multiplexing by combining FDD for under 6 GHz Frequencies, and TDD for mmWaves. They aim at optimizing the spectral efficiency on the downlink for better throughputs, and the sending power on the uplink for a better latency for time-sensitive applications. Hossain and Ansari, however, only consider a single gNB. The considered optimization issue is solved using Mixed Integer Non Linear programming (MINLP). But the objectives of this work are much reduced than ours given the limited variety of QoS affordable, and the lack of cooperation enabling. Zambianco and Verticale [23] also aim at optimizing the use of resources on a single gNB by limiting intra-slices interferences. For that, the issue is solved using Deep Reinforcement Neural networks (DRN) that converge to a solution that does not reach the optimal solution. This result seems to exhibit the limits of learning approaches compared to traditional optimization techniques like integer linear programming or constraint programming that easily converge to the optimal solution. In addition, the simple issue addressed by Zambianco and Verticale does not take into account scalability issues, and cooperation enabling between gNBs. Khodapanah et al. [24] adopts a similar approach based on reinforcement learning. But it also lacks enforcing isolation between slices, as authors propose a dynamic shared resources allocation. Raftopoulou and Litjens [25] and Korrai et al. [26] address similar issues related to the slicing interest or the spectral efficiency, but are far from addressing the issues in all their dimensions (i.e. Orthogonality, satisfaction, scalability and cooperation enabling). In addition, these two works try to solve the issue by simulation, and then without any proof that they consider all cases, and that they reach any optimal solution. Other works [27–29] are addressing the QoS enforcement problem in 5G networks, not in optimising radio resource allocation, but focusing on the network functions placement.

Few work has been done in multi-gNB system. Netshare [30] and AppRAN [31] frameworks are based on a centralized controller that decides the amount of resources to be allocated for each tenant on each gNB. Then, the slice resources allocation is executed on each gNB. Thus, the systems ensure isolation at best from packet-level. Also, they did not take the RAN slicing cooperation enabling requirement in their approaches.

On the other hand, the contribution in [32] sheds light on four approaches for the radio resources management from multi-cell multi tenant perspectives. Although, the fine grained resource management is covered to mitigate inter-slice interference, they did not propose any algorithm to enforce their approach. Zambianco and Verticale [33] have formalised a multi-objective function that minimizes the inter-slice interference in 5G networks with the assurance that

the slices will be isolated from each other. Nevertheless, the Scalability and satisfaction requirements are not taken into consideration.

D'oro et al. [10] proposed an algorithm to enforce the RAN slicing policies with interference mitigation. This is enabled through guarantying that the same (or similar in time/frequency) resource blocks (RB) are assigned to the same slices when gNBs are close enough to interfere among themselves. Although, their approach is efficient from interference mitigation perspective in 4G networks, it might be ineffective in resource utilization in the 5G system with the presence of different numerologies. Also, their work targets only orthogonality, satisfaction and cooperation enabling requirements. Thus, the scalability requirement is not considered. Moreover, contrarily to [10] that performs the allocation over two interfering gNBs basis, our work aims to an allocation from a multi-cell perspective, i.e. proceeding toward real 5G network deployment. Mei et al. [34] propose a framework for RAN slicing in 5G-beyond and 6G networks. In this framework, the RAN slicing is tackled over three levels : network, gNB and packet slicing level. So the large scale would be taken into consideration as well as small one (gNB and resources). The objective is to have a self-learning RAN slicing control over the three levels. Overall, it is an interesting proposition in favor of an autonomous system, but without any implementation/ simulation.

Overall, the work discussed in this article differs from existing work in that the RAN slicing enforcement is tackled in a multi-cell multi-slice perspective adapted to 5G system. We propose a new formulation of the RAN slicing enforcement problem that handles the slicing requirements in terms of orthogonality, scalability, satisfaction and cooperation enabling.

## 4 System design and model

Considering the RAN slicing requirements to achieve the 5G objective of serving diverse QoS slices (e.g. ultra-low latency (URLLC) slices, high-throughput slices, ...), we proceed to the system design of this work. The implementation of SDN at the RAN part (SD-RAN) is considered as one of the 5G enablers. Therefore, the system design in this work highlights the 5G RAN vision where the RAN is controlled in a centralized manner with an SD-RAN controller. This is crucial, as a cooperation between gNBs is required for a global resources allocation. Moreover, another fundamental element in 5G system is the flexibility at the physical layer compared to previous generations (e.g. 4G). This flexibility is enabled through the introduction of different numerologies at the radio resources level. As an illustration, to assure the URLLC slices sensitivity to latency, a numerology  $\mu$  with the lowest time slot duration would be more adapted for this slices type. Furthermore, the presence of the flexible resource structures (i.e. numerologies) involves a fine grained resource management. Therefore, we propose a new manner to decompose the radio resources grid to fulfill the allocation. Further, we investigate the possibility of deploying

the already discussed optimal allocation strategies. System models are then depicted.

### 4.1 System design

Let consider a set of gNBs covering a geographical zone. The 5G base station is named gNB. The gNBs cluster is controlled by a centralized SD-RAN controller, as illustrated in Fig. 4, noted  $R$ . This is essential to the high cooperation level required between the gNBs. The SD-RAN controls the RAN traffic, e.g. it receives the slices demand on each gNB (5G Base station) and all the RAN signaling information. We assume that SD-RAN copes with the scheduling and radio resources allocation over the specific zone. With the advanced implementation of intelligence in the radio part, the estimation of the slice traffic demand is possible, as illustrated for instance by Sciancalepore et al. [35] using measured deviations on the traffic, or Perez-Romero et al. [36]. On the other hand, several researches have been interested in the slicing profile generation, i.e. the slice demand and resources assignment [6, 37]. Therefore, the slicing profile is considered as an input argument for our system.

Furthermore, we propose to take advantage of the RAN intelligence in the 5G and the upcoming cellular networks to build a proactive allocation system for slices resources. In other words, with the pre-knowledge of the slices demand over the gNBs set, the SD-RAN proposes a resource allocation for the upcoming 10 ms, which corresponds to the frame duration in 5G cellular networks. This process is then run continuously every 10 ms to provide an autonomous resource allocation process for the global 5G network.

On the other side, with the different tile structures proposed by the 5G, an efficient resource management involves a fine grained access to the resources. For that, other than the 3GPP block decomposition, we propose a new scheme for the resources grid decomposition as explained in the following.

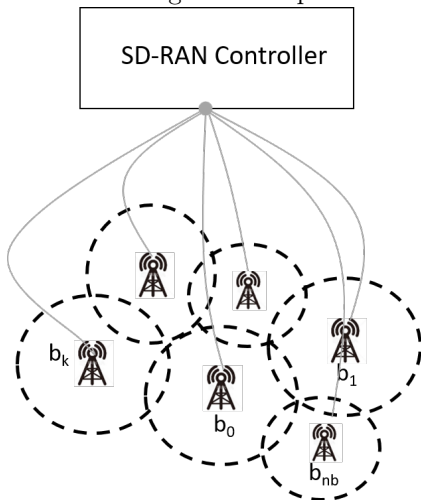


Fig. 4: System design

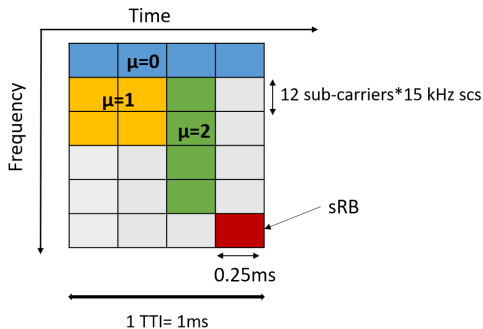


Fig. 5: Resource grid decomposition

### 4.1.1 Radio resources grid decomposition

With the diverse services flows and the increasing demand of cellular traffic, the 3GPP emphasizes the importance of treating the 5G radio resources differently from the earlier standards. For that, it introduces different numerologies on each frequency band. Each numerology is efficient for a specific service flow, particularly, the  $\mu = 2$  is much required for services with low latency. In the same perspective, we push this flexibility a step forward, and propose to handle the radio resources at small time and frequency granularities.

To that end, each gNB is entitled by its resource grid. With the variety of numerologies, we consider a resource grid decomposed into the smallest granularity in time and frequency. For instance, for the sub-6 GHz bands, where  $\mu$  can take values in  $\{0, 1, 2\}$ , the smallest resource block (sRB) is of size  $180 \text{ kHz} \times 0.25 \text{ ms}$ . Fig. 5 illustrates a decomposition for a small resource grid of 1 ms over 1.4 MHz. Three tile structures are considered. Namely, the tile structure for a given slice with  $\mu = 1$  is a square of  $2 \times 2$  sRBs.

The proposed resource grid decomposition allows a fine grained manipulation of the available resources, as they are shaped based on the slices numerologies requirements. Moreover, this decomposition results in an efficient control and management of the scarce radio resources. Also, it eases the way for the tight cooperation required by the 5G advanced techniques.

### 4.1.2 Objective formulation

Given the SD-RAN controller of a given zone, each gNB is characterized by its decomposed radio resource grid. For a specific allocation window, each slice is assigned an amount of tiles on each gNB over the RAN and the SD-RAN proposes an allocation for the slices tiles taking into account both of the following objectives:

The first objective aims to maximize the placement of the tiles in the resource grid with respect to the gNBs set, i.e. the maximization of the number of allocated tiles in the same or similar position (time/frequency), for each slice, over the gNBs set. This is because of the tight cooperation and coordination involved over the RAN for the 5G advanced techniques deployment as explained in Fig. 3.

Moreover, while allocating the slices tiles, an efficient radio resources utilization in each gNB is required. The latter could be achieved by an allocation that minimizes the sparse wasted unallocated resources. Or from another vision, maximizes the largest continuous unallocated resources space of each resource grid. Such allocation allows the MNO to scale up/down slices demand and also accept new slice requests (i.e. scalability) through reusing the largest unallocated resources portion. Thus, the objective is implicitly multi-objective.

This multi-objective allocation strategy, combining space and position optimization, assures an enforcement of the RAN slicing. In order to reach the

optimal solution of this multi-objective problem, we propose to attain the optimal solution for each objective separately. Then, three heuristics are depicted for simultaneous resolution.

## 4.2 System Model

Let denote  $B = \{b_1, \dots, b_{n_b}\}$  the cluster/set of  $n_b$  gNBs covering a geographical area. Notice that the gNB might offer macro as well as small cell coverage. They are controlled by a centralized Software Defined RAN (SD-RAN) controller  $R$ , as illustrated in Fig. 4. The multiple gNBs are adjacent to cover efficiently the geographical area. Such adjacency is highly vulnerable to interference. In 4G networks, this vulnerability is mitigated through the deployment of specific transmission techniques either within the RAN ( e.g. the Inter-cell Interference coordination (ICIC) or within the UEs by adapting the receiver diversity techniques. On the other hand, in 5G context, two levels of interference have to be mitigated : the inter-slices as well as the intra-slice interference. Thus, evolving the already-existing techniques or/and developing new ones is indispensable to fulfill the 5G requirements explained in 1.

Let us consider that  $R$  receives  $n_s$  slice requests to be served simultaneously during the allocation window  $T$ ,  $S = \{s_0, s_1, \dots, s_{n_s}\}$ . Based on the slices requirements on each gNB,  $R$  generates the slicing profile  $\Gamma = (\gamma_{s_i, k}^\mu)_{s_i \in S, k \in B}$ , where  $\gamma_{s_i, k}^\mu$  is the amount of tiles to be allocated to slice  $s_i$  in gNB  $b_k$  with numerology  $\mu$  during  $T$ . Each slice  $s_i$  is supposed to have the same numerology  $\mu$  over  $B$ , but requests a different amount of resources on each gNB, i.e. different slices have different numerologies  $\mu$  over  $B$ . As the generation of the slicing profile  $\Gamma$  has been already investigated by many researchers [6, 12, 37–39], it is considered as an input argument in our system model taking the resources grid size as the upper limit. Therefore, once it is generated in our work, it is primary to test its feasibility before the allocation process. In other words, a verification step of the possibility to allocate all the assigned slices resources in the appropriate gNB resource grid is required. In the following, we propose an exact method with an underlying constraint programming (CP) approach to test the slicing profile feasibility and tiles placement objective. A constraint problem is stated as a set of variables, where each variable has a finite domain of values, and a set of relations on subsets of these variables. CP eases the resolution of discrete problems through high level constraint propagation and controlled search behaviors [40].

### 4.2.1 Slicing Profile Feasibility Model (SPFM)

Let  $g_k = (r_{k, x, y})_{0 \leq x \leq N_r, 1 \leq y \leq T}$  be the matrix representing the resource grid of gNB  $b_k$ ,  $k \in \{0, \dots, n_b\}$ , with  $T$  and  $N_r$  representing the number of temporal

**Table 2:** System Model variables

Variable	Meaning
$T$	Time allocation window (number of temporal slots (0.25 ms))
$N_r$	Number of frequency channels of size 180 KHz
$\mu$	5G Numerology varies from 0 to 2
$R$	SD-RAN controller
$B = \{b_1, \dots, b_{n_b}\}$	Cluster/set of gNBs
$b_k$	gNB $k$ , $k \in \{1, \dots, n_b\}$
$n_b$	Total number of gNBs in set B
$S = \{s_0, \dots, s_{n_s}\}$	Set of slices requests
$s_i$	Slice number $i$ , $i \in \{0, \dots, n_s\}$
$n_s$	Total number of slices requests in S
$\Gamma$	The slicing profile
$\gamma_{s_i, k}^\mu$	Amount of tiles to be allocated to slice $s_i$ in gNB $b_k$ with numerology $\mu$ during $T$
$g_k$	Resource grid of gNB $b_k$
$k, x, y$	sRB in gNB $b_k$ with position (x,y)
$\zeta_{s_i}$	Set of tiles requested by slice $s_i$ over B
$\tau_j$	Tile of slice $S_i$ in a given gNB
$X_{b_k, s_i, j}$	Representation of $\tau_j$ of slice $s_i$ in gNB $b_k$ over X axis (frequency axis)
$Y_{b_k, s_i, j}$	Representation of $\tau_j$ of slice $s_i$ in gNB $b_k$ over Y axis (time axis)
$\alpha_{x, b_k}^j$	Starting point of interval variable $X_{b_k, s_i, j}$ over axis X
$\beta_{x, b_k}^j$	Ending point of interval variable $X_{b_k, s_i, j}$ over axis X

slots (0.25 ms) and frequency channels of 180 kHz respectively, i.e.  $r_{k,x,y}$  symbolizes the sRB in gNB  $b_k$  in position (x,y).<sup>2</sup> The resource grid size is therefore  $A = N_r * T$ .

A slicing profile  $\Gamma$  is considered as feasible, if all the tiles assigned to a group of slices on a given gNB  $b_k$  can be allocated over  $g_k$  without any overlapping, for all  $k \in \{0, \dots, n_b\}$ .

Let  $\zeta_{s_i} = \{\tau_j \text{ for } j \in \{0, \dots, \gamma_{s_i, k}^\mu\} \forall b_k \in B\}$  be the set of tiles requested by slice  $s_i$  over B. Each tile has a form of a rectangle based on the slice numerology (see Fig. 5). From that, we represent each tile  $\tau_j$  of slice  $s_i$  in gNB  $b_k$  by two interval variables  $X_{b_k, s_i, j}$  and  $Y_{b_k, s_i, j}$ . They refer to the tile allocation over frequency and time axis respectively. The length of the intervals is fixed as to reproduce the rectangle form of the tile. Particularly, if the tile  $\tau_j$  corresponds to a slice resource with  $\mu = 2$ , the length of  $X_{b_k, s_i, j}$  and  $Y_{b_k, s_i, j}$  are fixed to 4 sRBs and 1 sRB respectively. Therefore, a non overlapping between

<sup>2</sup>In this work, the sub-6 GHz band is selected for illustration purpose, but it is similar to the above-6 GHz band, where the sRBs will be of size (1440 kHz\*62.5 $\mu$ s).

two tiles  $\tau_j$  and  $\tau_h$  on a given  $g_k$  refers to their non overlapping over X and Y axis, i.e.  $X_{b_k, s_i, j} \cap X_{b_k, s_i, h} = 0$  and  $Y_{b_k, s_i, j} \cap Y_{b_k, s_i, h} = 0$ .

Let  $\alpha_{x, b_k}^j, \alpha_{y, b_k}^j$  be the variables referring to the starting point of the two intervals  $X_{b_k, s_i, j}$  and  $Y_{b_k, s_i, j}$  respectively. And  $\beta_{x, b_k}^j, \beta_{y, b_k}^j$  point out their ends. Tab.2 summarizes the introduced variables in this work. The SPFM can be therefore formulated using CP approach as follows:

$$\alpha_{x, b_k}^j \leq N_r \quad \forall b_k \in B \quad \forall j \in \zeta_{s_i} \quad \forall s_i \in S \quad (1)$$

$$\alpha_{y, b_k}^j \leq T \quad \forall b_k \in B \quad \forall j \in \zeta_{s_i} \quad \forall s_i \in S \quad (2)$$

$$\begin{aligned} & (\alpha_{x, b_k}^j \geq \beta_{x, b_k}^r \vee \alpha_{x, b_k}^r \geq \beta_{x, b_k}^j) \wedge \\ & (\alpha_{y, b_k}^j \geq \beta_{y, b_k}^r \vee \alpha_{y, b_k}^r \geq \beta_{y, b_k}^j) \quad \forall r, j \in \zeta_{s_i} \quad \forall b_k \in B \end{aligned} \quad (3)$$

The constraints 1 and 2 limit the allocation bounds of each tile over both X and Y axis respectively. Then, the second constraint 3 ensures the allocation of the required slices tiles on each gNB without any overlapping between two tiles. This way the model is feasible when all the slices demands in a given gNB are allocated to the appropriate resource grid.

For feasibility model (SPFM) implementation, the IBM CPOptimizer constraint programming solver IBM ILOG (CPO)<sup>3</sup> is used. It provides a high level scheduling constraints. The allocation of tiles taking into consideration the constraint 3 can be directed by the *SetSearchPhase* function. It guides the search for positions with *SearchPhase* over X-axis and Y-axis for each tile with respect to non-overlapping constraint. Let  $VX_k$  denotes all the interval variables over X-axis representing the tiles assigned for the allocation on  $b_k$ , and  $VY_k$  the ones over Y-axis. The use of *searchPhase* is therefore written as:

$$\begin{aligned} & \text{SetSearchPhases}(\text{searchPhase}(VX_k), \\ & \text{searchPhase}(VY_k)) \quad \forall b_k \in B \end{aligned} \quad (4)$$

Once the SPFM is verified and the slicing profile is feasible (i.e. otherwise it is rejected), a RAN slicing enforcement policy  $\psi$  is required to fulfill the requirements depicted in section 1. It should lead to an optimal radio resources allocation over the  $b_{n_b}$  gNBs.

As stated earlier, the problem is treated as a Multi-Objective Optimisation Problem (MOOP). One objective carries the maximization of slices' tiles placement in the same frequency-time position in the resource grid of the adjacent gNBs. The other objective deals with the maximisation of the largest unallocated continuous portion of radio resources on each gNB. In the following,

---

<sup>3</sup>CPLEX Optimization studio 12.9: <http://www.cplex.com>



the radio resources placement objective is modeled with an exact optimization method. And, the approach followed to carry the largest continuous unallocated space during the resources allocation is explained.

#### 4.2.2 Enforcement of Slice Resources Placement (ESRP)

The policy  $\psi$  has the objective to maximize the tiles placement of a given slice in the same position over the set of gNBs,  $B$ . For that we introduce the notion of tied tile.

**Definition 1** (Tied tile). *A given tile  $\tau_j$  is tied to a slice  $s_i$  over a gNBs set  $B$  if and only if the tile  $\tau_j$  is placed in the same position over all the gNBs in the cluster  $B$ , i.e.  $\tau_j$  has the same frequency and time position on each  $g_k, \forall b_k \in B$*

Each tile  $\tau_j$  of slice  $S_i$  in gNB  $B_k$  is represented by two interval variables  $X_{b_k, s_i, j}$  and  $Y_{b_k, s_i, j}$  as explained in 4.2.1. With  $\alpha_{x, b_k}^j, \alpha_{y, b_k}^j$  are the variables indicating the starting point of the two intervals  $X_{b_k, s_i, j}$  and  $Y_{b_k, s_i, j}$  respectively, and  $\beta_{x, b_k}^j, \beta_{y, b_k}^j$  their ends. With that, a tile is tied if and only if  $\alpha_{p, b_k}^j = \alpha_{p, b_{k'}}^j$  and  $\beta_{p, b_k}^j = \beta_{p, b_{k'}}^j \forall b_k \in B, p \in \{x, y\}$ .

In other words, a tile of a given slice is tied if all its sRBs are allocated in the same position over the set of involved gNBs, i.e. gNBs where tile  $\tau_j$  is present, as the slice demand varies over the gNBs. Consequently, we introduce the concept of tied sRB:

**Definition 2** (Tied sRB). *A given sRB  $r_{k, x, y}$  is tied to a slice  $s_i$  over  $B$  if and only if the sRB is allocated to the same slice over each gNB in  $B$ , i.e.  $(x_k, y_k) = (x_{k'}, y_{k'}) \forall b \in B$ .*

Even-though the allocation is performed per tile, it is clear that the maximization of the total amount of tied tiles for all the slices turns out to the maximization of the total amount of tied sRBs for all the slices, i.e. a tile is composed of 4 contiguous sRBs. Accordingly, we model mathematically the system as to maximize the total amount of tied sRBs. The model is depicted in the following.

- **ESRP model**

For a given tile  $\tau_j$  of  $s_i$ , let denote  $\theta_j$  the amount of its tied sRBs over  $B$ . As each tile  $\tau_j$  is symbolized by two interval variables on each  $g_k$ ,  $X_{b_k, s_i, j}$  and  $Y_{b_k, s_i, j}$ ,  $\theta_j$  corresponds to the overlap length between both intervals over all the involved gNBs. It can be formulated as follows:

$$\theta_j = \Pi_{p \in \{x, y\}} (\Psi_p^j - \Upsilon_p^j)$$

Where  $\Psi_p^j = \min_{\forall b_k \in B_j} \beta_{p,b_k}^j$  and  $\Upsilon_p^j = \max_{\forall b \in B_j} \alpha_{p,b_k}^j$ ,  $p \in \{x, y\}$ , identify the start and end position of the overlap between the rectangles over the involved gNBs over both frequency and time axis. It is worth noting that the overlap score between two intervals  $I_1$  and  $I_2$  is given by the CPO function *OverlapLength*, i.e.  $OverlapLength(I_1, I_2)$ . Such function returns the length of overlap between two intervals  $I_1$  and  $I_2$ . By way of illustration, let us consider the allocation over two gNBs of tile  $\tau_j$  with  $\mu = 2$  as shown in Fig. 6. Let suppose that both tiles have the same y-axis position. The amount of tied sRBs is exactly the surface of the overlap between the  $\tau_j$  in gNB  $b_0$  and  $\tau_j$  in gNB  $b_1$ . The starting point of this surface over each axis can be computed by  $\max(\alpha_{p,b_0}^j, \alpha_{p,b_1}^j)$  and the end position by  $\min(\beta_{p,b_0}^j, \beta_{p,b_1}^j)$ . On the X-axis, they are equal to  $\alpha_{x,b_0}^j$  and  $\beta_{x,b_1}^j$  respectively. Thus, it represents two sRBs, i.e.  $\theta_j = 2$ . That is, two sRBs are tied between the two gNBs.

Therefore, the total tied sRBs for a given slice  $s_i$  over  $B$  is given by:

$$\Theta_{s_i} = \sum_{j \in \zeta_{s_i}} \theta_j$$

Further, the total tied sRBs over  $B$  can be expressed as the summation of the total tied sRB of each slice over  $B$ :  $\chi = \sum_{s_i \in S} \Theta_{s_i}$

The objective is then formulated as to find the slicing enforcement policy  $\psi$  that maximizes  $\chi$ ,  $\Psi$  is the set of all possible policies. It is developed with a constraint programming (CP) approach as the SPFM (section 4.2.1) resolution. In the CP implementation, the constraints are explicitly stated to shape the aimed solution, i.e. in this case the maximization of  $\chi$ .

$$\max_{\psi \in \Psi} (\chi) \quad (\text{ESRP})$$

subject to

$$\alpha_{x,b_k}^j \leq N_r \quad \forall b_k \in B \quad \forall j \in \zeta_{s_i} \quad \forall s_i \in S \quad (5a)$$

$$\alpha_{y,b_k}^j \leq T \quad \forall b_k \in B \quad \forall j \in \zeta_{s_i} \quad \forall s_i \in S \quad (5b)$$

$$\sum_{j \in \zeta} \theta_j \leq \gamma_{s_i,k}^\mu \quad \forall k \in B \quad \forall s_i \in S \quad (5c)$$

$$\alpha_{x,b_k}^j \geq \beta_{x,b_k}^r \vee \alpha_{x,b_k}^r \geq \beta_{x,b_k}^j \wedge \quad (5d)$$

$$\alpha_{y,b_k}^j \geq \beta_{y,b_k}^r \vee \alpha_{y,b_k}^r \geq \beta_{y,b_k}^j \quad \forall r, j \in \zeta_{s_i} \quad \forall b_k \in B$$

$$\Psi_p^j \geq \Upsilon_p^j \quad \forall p \in \{x, y\} \quad \forall \tau_j \in \zeta_{s_i} \quad \forall s_i \in S \quad (5e)$$

The constraints (5a) and (5b) ensure that all the allocated tiles are inside the resource grid, i.e. the allocation does not outpace the gNB grid

limits on both frequency (5a) and time (5b) axis. The second constraint (5c) guarantees that each slice receives at maximum its required amount of tiles over each gNB. Then, the constraint (5d) addresses the resource isolation by assuring the non overlapping between tiles on the same gNB, i.e. each sRB is allocated at maximum to one slice. Hence, the slices orthogonality is achieved. Then, the last constraint (5e) assures the non negativity of each tied sRB surface.

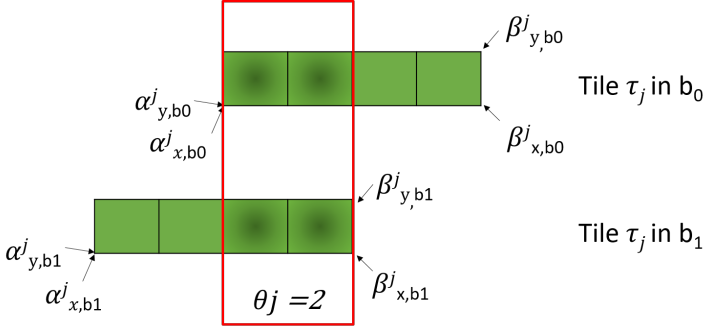


**Fig. 6:** Illustration of tied sRBs of a tile between two gNBs

### 4.2.3 Maximization of the Continuous Unallocated Space (MCUS)

The second objective targets the maximization of the continuous unallocated space on each gNB resource grid  $g_k$ ,  $k \in B$ . For that, the problem is tackled as a two-dimensional rectangle bin packing (2DBP) optimization problem. In such problem, given a sequence of rectangular objects with specific height and width, the objective is to place the maximum of these objects inside a minimum bins of fixed size, with the constraint of no-overlapping between the rectangles. The NP-Hardness of this problem is proven by a reduction from the 2-partition problem [41].

Let project the 2D bin packing to the context of the resource allocation with MCUS objective. In our case, the rectangular objects to pack in the bins are the slices tiles with their specific numerologies  $\mu$ . Each tile  $\tau_j$  has a form of a rectangle based on the slice numerology. Particularly, the tiles of a given slice with numerology  $\mu = 2$  have a rectangular form of width and height equal to 4 and 1 respectively. Each gNB decomposed resource grid  $g_k$  is represented by a bin. It is supposed that the bins have the same size over all the gNBs set  $B$ , i.e.  $\forall k \in B \quad size(g_k) = A$ . Only one bin is available for the packing for each gNB. Its size is exactly the size of the resource grid in terms of time and frequency resources, i.e. allocation time over the carrier bandwidth. This can be considered as Knapsack use case problem of 2DBP.

The Knapsack problem is argued to be NP-hard. The achievement of the MCUS objective is then also NP-hard. Over decades, several algorithms are proposed in the literature to approximate the optimal solution for 2DBP. They include the Skyline algorithm proposed in [42]. It starts by placing the first rectangle object in the bottom left (BL). Then, each new rectangle object is left-aligned on top of the skyline level that results in the top side of the object lying at the bottom-most position of the bin. The topmost edges of already packed objects is tracked as illustrated by the red line in Fig. 7. The example shows the packing of 6 tiles with  $\mu = 1$  and 5 tiles with  $\mu = 0$  using the skyline algorithm. The algorithm then maintains the list of these horizons or "skyline" edges. The later grows linearly in the number of the packed rectangle objects. And for each rectangle packing top of a hole, it is possible and easy to compute the free rectangle that would be lost after packing. Thus, it is stored and evaluated for an aforementioned use. Such approach is referred as a waste map (WM) improvement for the skyline (BL) heuristic.

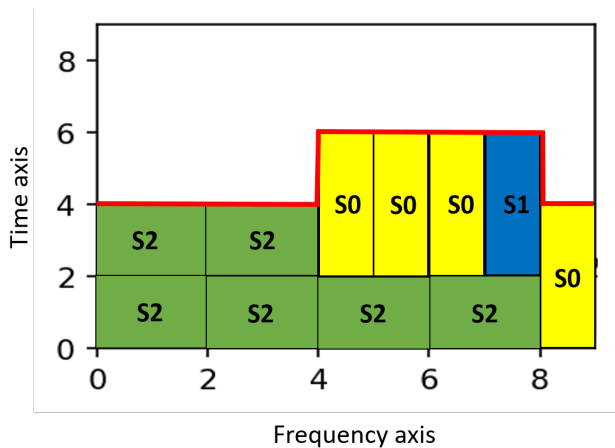


**Fig. 7:** Illustration of Skyline algorithm packing 3 slices tiles

The authors tested a benchmark of 2DRP heuristics and variants of the skyline algorithms. They proved that skyline-BL-WM outperforms all the best tested online packers, in terms of packing efficiency as well as the run-time performance, when packing to one bin at a time. As the algorithm packs the objects in a way to minimize the wasted space between the packed objects, it results in letting the largest unallocated space. Therefore, the skyline-BL-WM heuristic is chosen to approximate the MCUS solution, for two reasons:

- The algorithm is highly performing in both time convergence and packing efficiency on one bin. This corresponds to the use case of this work, i.e. each  $g_k$  is represented by one bin and the allocation is allowed only in this bin.

- The algorithm approach seeks to pack the objects (tiles) as to have the lowest skyline (contour). This is advantageous, as we are seeking to let the maximum of unallocated space over time axis. Hence the bottom could be chosen as the frequency axis. The skyline is then aligned over time as shown on Fig. 7. This way, the allocation of different tiles numerologies could occupy the continuous unallocated space, e.g. serving the sudden delay-critical requests. Thus, the scalability requirement is assured.

The Skyline heuristic approximates the MCUS solution. Thus, there is a need to evaluate its performance. For that, an optimal score is necessary. In this work, the naive method that encounters the Largest Continuous Unallocated Space (LCUS) topmost upper bound is used, as depicted in the following. It is therefore considered as the optimal LCUS solution, in the same way as it has been demonstrated in [42].

**+LCUS topmost upper bound (LTUB):** On a given resource grid  $g_k$ ,  $k \in B$ , the topmost LCUS upper bound can be achieved when all the tiles of all the slices are allocated without overlapping and without space left in between, i.e. non existence of wasted space between allocated tiles. The size of each resource grid can be computed, as stated before, by  $A = N_r * T$ , where  $N_r$  is the number of frequency channels and  $T$  the allocation window.  $A$  refers also to the total number of available sRBs on each  $g_k$ . Given the slices demand  $\gamma_{s_i,k}^\mu$  in terms of tiles, the total required tiles on each  $b_k$  can be computed by:  $\rho_k = \sum_{s_i \in S} \gamma_{s_i,k}^\mu$ . Therefore, the total allocated sRBs on each  $g_k$  equals  $4 * \rho_k$ , as each tile contains 4 sRBs. From that, the highest upper bound of LCUS, noted  $LCUS_k$ , can be quantified by  $LTUB_k = A - 4 * \rho_k$ . The topmost upper bound over all  $B$  is then:  $LTUB = \sum_{k \in B} LTUB_k$ .

## 5 Models evaluation

In the previous section, the two objectives are modeled separately. The model evaluation is necessary. The second objective is treated as a 2DBP optimization problem. With the NP-hardness of such resolution, the skyline heuristic is used for this resolution. In order to evaluate its performance in term of LCUS, the LTUB is taken as the optimal solution. In this section, the evaluation of both objectives solutions is conducted. The metrics of this evaluation are: the total tied sRBS (TTR) for ESRP, the LCUS for skyline and the convergence time for all algorithms (i.e. ESRP and Skyline).

### 5.1 Performance metrics computation

#### 5.1.1 Convergence Time (CT)

For CPO models, the CT is computed with time function, and time limit is fixed to 600 s. For skyline, python time module is used.

### 5.1.2 Total tied sRBs (TTR)

The objective behind the implementation of the ESRP model is to maximize the total tied sRBs during an allocation of slices set over a gNBs set. Therefore, the basic evaluation metric is the achieved total tied sRBs, noted TTR. If the model does not reach the optimal TTR score during the 600 s, the compilation is stopped and the upper bound score is saved as optimal score. Otherwise, the objective score is retained. In both cases, TTR is extracted directly as an output from the optimization model.

### 5.1.3 Largest Continuous Unallocated Space (LCUS)

In order to count the largest continuous unallocated space (LCUS) after each allocation, we derive a binary matrix from the resource grids after the allocation completion, i.e. each allocated sRB to a given slice corresponds to an element matrix with value equals 1 and the unallocated sRBs (elements) worth 0. Then, we apply the Connected Component Labeling (CCL) with the Depth First Search (DFS) method [43] on each binary matrix. A connected component in a matrix is the subset of matrix elements with same value, where each element is reachable by the other elements. Thus, in our case the LCUS is exactly the maximum subset of zeros among each matrix, i.e. continuous unallocated sRBs.

## 5.2 ESRP evaluation: Slice Resources Placement Problem

For this work evaluation, we consider a time allocation window corresponding to the 5G radio frame duration, i.e. 10 ms and a frequency bandwidth of 5 MHz. Based on the proposed resource grid decomposition shown in Fig. 5, each TTI of 1 ms is decomposed into 4 time slots of 0.25 ms, hence  $T = 40$  in this case. Also, the smallest frequency grain in the resource grid is fixed to 180 kHz, thus,  $N_r = 27$ . Further, the resource grid size in all simulations is:  $N_r = 27$  and  $T = 40$ . For each test, the number of slice requests and the number of adjacent gNBs are fixed. The slicing profile  $\Gamma$  is randomly generated for each simulation run as to have at maximum 80% of the grid usage. Thus, a maximum of 80% of the resources grid per gNB is distributed randomly between all the slices requests in that gNB. As already stated, the slicing profile generation is out of the scope of this work and considered as an input system. Further, 100 independent simulation runs are realized for each given test. Each test has a fixed size of slices and gNBs sets, and different slicing profile. Six B set sizes and seven slices sets have been tested. Thus, a total of 4200 simulation runs is performed in this work. For each simulation run the model feasibility (SPFM) is tested and the infeasible slicing profiles are rejected. In case of its feasibility, the same instances are used for ESRP model and skyline. Otherwise, a new slicing profile is generated. The results are then averaged over all the simulations runs for each test.

### 5.2.1 Total Tied sRBs (TTR)

Fig. 8 and Fig. 9 illustrate the optimal/upper bound TTR score for the ESRP model. Fig. 8 depicts the optimal/upper bound TTR score as a function of B size serving 3 slices, while Fig. 9 depicts this TTR score as a function of S size for a system with 3 gNBs. The TTR score is increasing with B size growth. Thus, larger B sets produces higher TTR scores (optimal/upper bound score) as expected. To give more insight to this result, let us consider two scenarios : (1) a system with two gNBs  $\{b_0, b_1\}$  and a slice  $s_0$  that should be allocated 2 tiles with  $\mu = 1$  on  $b_0$  and 4 tiles on  $b_1$ , (2) a system with 3 gNBs  $\{b_0, b_1, b_2\}$  and a slice  $s_1$  that should be allocated 2 tiles with  $\mu = 1$  on  $b_0$ , 4 tiles on  $b_1$ , and 5 tiles on  $b_2$ . In scenario (1), the maximum tiles that could be tiled is 2 (i.e. allocated in the same position over both gNBs). Hence, the optimal/upper bound TTR in this case is 8 sRBs (i.e. each tile is composed of 4 sRBs). In the second scenario with a larger set of gNBs, the maximum tiled tiles over the three gNBs is 2, then 2 tiles and 3 tiles are still remaining to be allocated over  $b_1$  and  $b_2$  respectively. In this case, another 2 tiles should be allocated over both gNBs ( $b_1, b_2$ ). Therefore, 16 sRBs (4 tiles) is the optimal/upper bound TTR in scenario (2). Thus, TTR has increased when increasing the B set size.

Furthermore, 5G aims to assure each slice QoS and hence enabling the appropriate advanced radio technique per slice (e.g. CoMP). The increase of TTR over larger B sets implies, at least, the adaptation of the required radio technique rapidly, i.e. when a served slice has new demand on other adjacent gNBs. The TTR enables the tight cooperation between the gNBs to implement the 5G advanced radio techniques, but its increase with higher gNBs might increase the complexity behind the system technique adaptation per slice.

Regarding S variation, a slight variation of TTR score is observed Fig. 9). This reflects the insensitivity of the model to the slices set growth with respect to TTR. However, the radio resource grid on each gNB remains with the same size when the number of slices demand increases. Hence the slicing profile is adapted adequately with respect to the slices set size. Also, it is worth mentioning that maximum slices set size (i.e. 15) is chosen as to avoid any counter-effect of centralization as it has been proven by authors in [44].

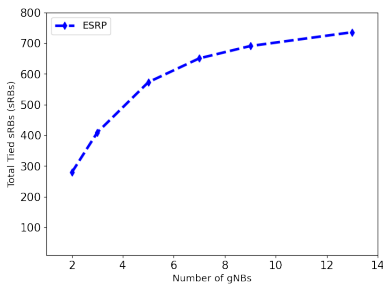


**Fig. 8:** ESRP TTR(sRBs) as a function of B.

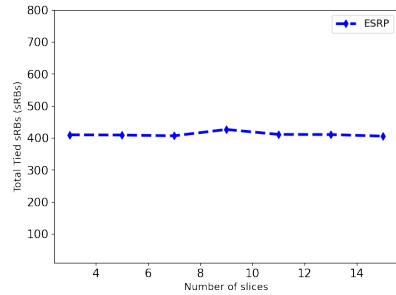


**Fig. 9:** ESRP TTR(sRBs) as a function of S.

It is worth noting that out of the total feasible simulation runs (4198), the successful optimal TTR is achieved only 15,55% with ESRP. Most of the optimal scores are reached for the small systems composed of 2 gNBs. Therefore, the model is unable to achieve the optimal TTR score for bigger systems within 600s.

### 5.2.2 Convergence Time (CT)

Fig. 10 and Fig. 11 plot the CT in seconds as function of the  $B$  size with different slices sets and  $S$  size with different  $B$  sets respectively. For small systems the model converges approximately in the order of hundreds of seconds. Then, the CT increases gradually with the  $B$  or  $S$  set size growth. For larger systems, the model CT reaches quickly 600 s that corresponds to the prefixed time limit.

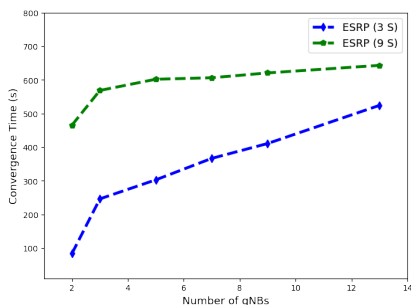


**Fig. 10:** ESRP models CT (s) as a function of  $B$  serving 3 and 9 slices.

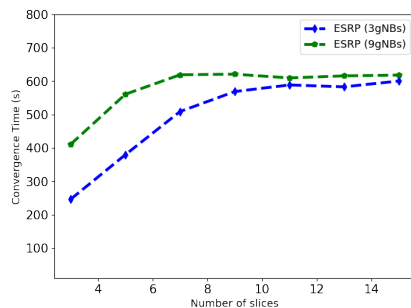


**Fig. 11:** ESRP models CT (s) as a function of  $S$  with 3 gNBs and 9 gNBs.

## 5.3 MCUS evaluation: Unallocated Space Problem

In this part, the achieved LCUS with skyline is compared with the upper bound LTUB, with respect to  $S$  and  $B$  sizes.

### 5.3.1 Largest Continuous Unallocated Space (LCUS)

Fig. 12 shows the variation of LCUS by skyline and LTUB as a function of  $B$  size in a system serving 3 slices. Over the different  $B$  sizes, the skyline heuristic reaches the topmost upper bound LCUS (LTUB). The two curves representing the LTUB and skyline score are similar. This reflects the capability of skyline to allocate efficiently the slices tiles without any space waste in between when the slicing profile is feasible. The LCUS is increasing with  $B$  size. This is expected, as the LCUS is the sum of  $LCUS_k$ ,  $k \in B$ , over  $B$ . Moreover, the LCUS varies slightly with  $S$  size variation for a system with 3 gNBs as shown on Fig. 13. With different  $S$  sets, the skyline always attain the LTUB. From that, LCUS skyline is sensitive to the number of served slices but always reaching the optimal score (LTUB). This is could be explained by the variety of slices



demand and their diverse numerologies for each test. In fact, the LCUS varies with the numerologies combination set that should be allocated at each test.

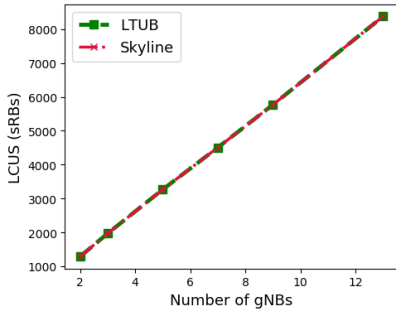


**Fig. 12:** LCUS (sRBs) for both Skyline and LTUB as a function of B set size.

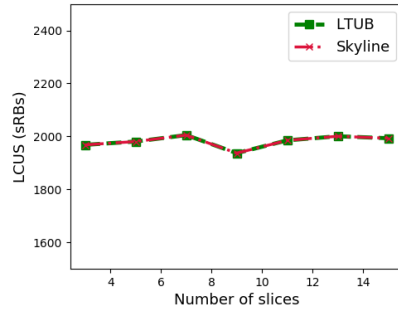


**Fig. 13:** LCUS (sRBs) for both Skyline and LTUB as a function of S set size.

### 5.3.2 Convergence Time (CT)

The skyline CT as a function of B size and S size is shown on Fig. 14. The skyline converges in the order of hundreds of milliseconds. The CT increases for B sets larger than 7 gNBs (Fig. 14 (a)). Nonetheless, it does not outpace 0.45 s. A small CT difference is remarked when serving 3 and 9 slices. It is zoomed out on Fig. 14 (b). From that, small set of slices (e.g. 3 slices) served over 9 gNBs induces higher CT. Such result could be explained by Skyline struggling to maximize the LCUS for higher number of resources with probably the same structure. However, higher number of slices comes with higher numerologies diversity, i.e. resources structures. Nevertheless, for lower gNBs set, the CT does not exceed 0.1 ms for different slices set sizes. Then, for larger B size, the CT is between 0.16 s and 0.45 s for the various S set size. Therefore, the skyline is interesting with respect to CT, as it can be implemented for SD-RAN real time allocations.

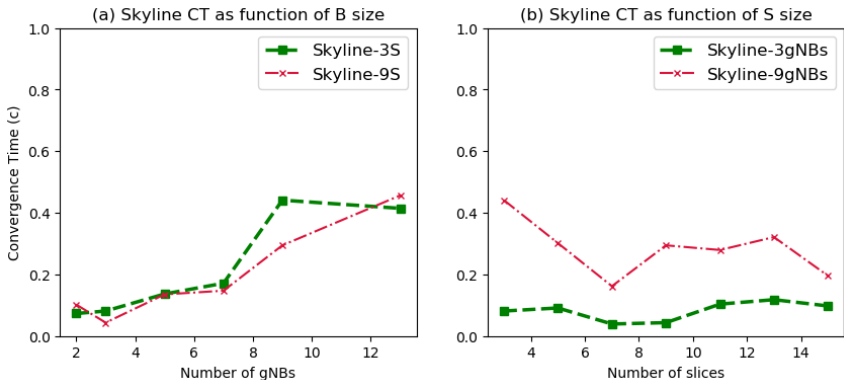


Fig. 14: CT for Skyline as a function of B set size (a) and S set size (b).

## 5.4 Discussion

Overall, the ESRP model converges slowly in the order of hundreds of seconds. This is with the fixed time limit for the simulations run, i.e. 600 s. Hence, ESRP might converge at higher time scales. Also, the percentage of finding the optimal TTR by the used of CP solver (CPLEX) within this time limit is feeble. It restricts its implementation for real time slicing. There is therefore a need for heuristics to achieve the cooperation enabling requirement rapidly.

On the other hand, the NP-hardness of the MCUS objective brought us to use the heuristic solution, especially the skyline heuristic. The later has demonstrated good performance in terms of largest continuous unallocated space that attains the topmost upper bound (LTUB) as well as a convergence time in less than 0.45 s for various B and S sets. This makes the skyline suitable for real time deployments of RAN slicing without enabling cooperation requirement.

With the aim of real time RAN slicing enforcement, an heuristic based solution seems to be the best choice, as the ESRP model converges slowly in the order of hundreds of seconds without taking into account the scalability requirement. Accordingly, we propose three heuristics to support the RAN slicing requirements.

## 6 Proposed heuristics

The aim of this work targets the real time RAN slicing enforcement. For that, an allocation strategy combining the maximisation of the total tied sRBs over a given set of gNBs as well as the largest continuous unallocated space is argued to reach such aim. The space maximization objective is discovered to be NP-hard. And, the developed ESRP models converge slowly. Thus, it limits the real time slicing enforcement. Therefore, we propose to tackle this multi-objective problem with heuristic based approach.

Given the multi-objective criterion, a compromise between both objectives is unavoidable. The slice owner might have the possibility to allocate its tied resources to the users at the cells boards highly affected by interference. Thus, it can enable the cooperation techniques on only these resources. Certainly, a slice with higher TTR is much more beneficial, as the slice owner would have more flexibility on its resources. On the other hand, the LCUS enables the scalability. Thus, the MNO can serve more slices. Moreover, an improvement of the current served slices QoS can be achieved by scaling up their resources. In addition, it allows a high level of spectral efficiency. Accordingly, The MCUS is prioritized in the heuristic development.

The aforementioned used skyline heuristic reaches the optimal LCUS in a small time scale, i.e. maximum 0.45 s. This is attractive from the real time implementation perspective. For such reason, the proposed heuristics use the skyline as an underlying allocation technique and three heuristics are developed as depicted in this section. With skyline approach, the LCUS is guaranteed while the TTR is targeted at best to find the optimal slicing enforcement policy.

## 6.1 Heuristic 1: Highest Slice First (HSF)

Each slice is assigned a different amount of resources on each gNB. Thus, the slices requiring higher amount of resources over B are expected to generate high number of tied sRBs. Considering such fact, the total required resources over B is computed for each slice based on the slicing profile  $\Gamma = (\gamma_{s_i,k}^\mu)_{s_i \in S, k \in B}$ , ( $\gamma_{s_i,k}^\mu$  is the amount of tiles to be allocated to slice  $s_i$  in gNB  $b_k$  with numerology  $\mu$  during  $T$ ) as follows:  $\lambda_{s_i} = \sum_{k \in B} \gamma_{s_i,k}^\mu$ .

The algorithm first tries to set the bigger slices at the same position in the interfering gNB. Therefore, the slices are sorted in a decreasing order based on  $\lambda_{s_i}$ . Hence, the slice with higher amount of tiles is first served and the lower last. We denote such method as the **Highest Slice First**, HSF. It is represented in Algorithm 1 and performs as follows:

- (i) ) compute the total required resources of all the slices over B,  $\Lambda = (\lambda_{s_i})_{s_i \in S}$ .
- (ii) ) sort the slices in decreasing order based on  $\lambda_{s_i}$  and generate the set  $S^o$  with ordered slices.
- (iii) ) insert the first object of the first slice in  $S^o$  in the bottom left of the bins.
- (iv) ) allocate the current slice object in the bottom-most position leaving the largest unallocated space over time in each bin and minimizing the wasted space between objects of same bin.
- (v) ) keep inserting the objects of the current slice on all the bins with respect to **iv** until the required objects of the current slice are allocated on all the bins.
- (vi) ) repeat **iv** and **v** as to allocate the slices in sequential order as in  $S^o$ , until all the objects of each slice on each gNB are allocated.

The first instructions of the total required resources computation and slices sorting run in  $O(n_b * n_s + n_s \log(n_s))$ . Let denote  $\rho$  the total required tiles of

**Algorithm 1** Heuristic1- HSF

---

```

1: Input: B, S,  $\Gamma$ 
2: Output: HSF sRBs allocation  $G^{HSF} = (g_k^{HSF})_{k \in B}$ 
3: set  $g_k^{HSF} = (\alpha_{k,f,t}^{s_i,\mu})_{f,t} = 0 \quad \forall k \in B \quad \forall s_i \in S$ 
4: Compute  $\Lambda = (\lambda_{s_i})_{s_i \in S}$ 
5:  $S^o \leftarrow$  sort S in decreasing order based on  $\Lambda$ 
6: for each gNB  $b_k \in B$  do
7:   for slice  $s_i \in S^o$  do
8:     while  $\gamma_{s_i,k} \neq 0$  do
9:       allocate  $s_i$  tile subsequent sRBs with LCUS account.
10:      update  $g_k^{HSF}$ 
11:      remove the allocated object from  $\gamma_{s_i,k}$ 
12:     end while
13:   end for
14: end for
15: end

```

---

all slices over all the gNBs, i.e.  $\rho = \sum_{s_i \in S} \lambda_{s_i}$ . The heuristic core code run in  $O(n_b * \rho^2)$ . This is because the packing time on each gNB is  $\rho^2$ , and, it is largely superior to  $n_b * n_s + n_s \log(n_s)$ . Consequently, the HSF converges with a time complexity of  $O(n_b * \rho^2)$ .

## 6.2 Heuristic 2: Iterative Minimum Allocation (IMA)

HSF allocates in sequential order all the tiles of a given slice over all the involved gNBs, starting with the slice requesting the highest total number of tiles over B.

Given that the slices request different amount of tiles over a set of gNBs, it is clear that the maximum tied sRBs between a subset of gNBs equals the minimum required resources over the same subset. For instance, let us consider a subset of three gNBs serving one slice  $s_1$  with numerology  $\mu = 0$ ,  $s_1$  requests 3 tiles on  $b_1$ , 2 tiles on  $b_2$  and 5 tiles  $b_3$ . The maximum tied sRBs over  $B = \{b_1, b_2, b_3\}$  for  $s_1$  equals 2 tiles, i.e. 8 sRBs as each tile is composed of 4 sRBs. Hence, to maximize the total tied sRBs over B we need to ensure the allocation of this minimum of  $s_1$  8 sRBs over B. In a general case with multiple slices, the maximization of the total tied sRBs over a subset of gNBs implies the assurance at best that the minimum required sRBs for each slice is allocated in the same time/frequency position over the gNBs subset. Thus, with the aim to maximize the total tied sRBs over B, we propose an iterative allocation of the non null minimum required tiles of each slice over the involved gNBs. We refer to such approach as an Iterative Minimum Allocation (IMA) approach.

Let denote  $m_{s_i}$  the non null minimum required objects for slice  $s_i$  over B. It is computed as follows:  $m_{s_i} = \min_{\substack{k \in B \\ \gamma_k^{s_i} \neq 0}} \gamma_k^{s_i}$ .

The IMA procedure works as follows:

- i ) compute the total required resources of all the slices over B,  $\Lambda = (\lambda_{s_i})_{s_i \in S}$ .
- ii ) sort the slices in decreasing order based on  $\lambda_{s_i}$  and generate the set  $S^o$  with ordered slices.
- iii ) Compute the minimum required objects for all slices,  $s_i \in S^o$  over all B,  $M = (m_{s_i})_{s_i \in S^o}$ .
- iv ) allocate  $m_{s_i}$  sequentially with leaving the LCUS over each bin.
- v ) update  $\gamma_{s_i,k}$  by subtracting  $m_{s_i}$ .
- vi ) repeat **iii**, **iv** and **v** for all  $s_i \in S^o$ . If  $\gamma_{s_i,k} = 0$ . Remove  $s_i$  from  $b_k$ .
- vii ) If  $\Gamma = 0$ , stop. Otherwise, repeat vi until all the slices are assigned the required tiles over B.

---

**Algorithm 2** Heuristic2-IMA
 

---

- 1: **Input:** B, S,  $\Gamma$
  - 2: **Output:** IMA sRBs allocation  $G^{IMA} = (g_k^{IMA})_{k \in B}$
  - 3: set  $g_k^{IMA} = (\alpha_{k,f,t}^{s_i,\mu})_{f,t} = 0 \quad \forall k \in B \quad \forall s_i \in S$
  - 4: Compute  $\Lambda = (\lambda_{s_i})_{s_i \in S}$
  - 5:  $S^o \leftarrow$  sort S in decreasing order based on  $\Lambda$
  - 6: **while**  $\Gamma \neq 0$  **do**
  - 7:     Compute  $M = (m_{s_i})_{s_i \in S^o}$
  - 8:     **for each** gNB  $b_k \in B$  **do**
  - 9:         **for each** slice  $s_i \in S^o$  **do**
  - 10:             add  $m_{s_i}$  to the allocation with LCUS
  - 11:             Update  $g_k^{IMA}$  by allocating  $m_{s_i}$  tiles subsequent sRBs
  - 12:             remove the allocated objects from  $\gamma_{s_i,k}$
  - 13:         **end for**
  - 14:         Update  $\Gamma$  by removing the allocated  $m_{s_i}$  objects from  $\gamma_{s_i,k}$
  - 15:         **if**  $\gamma_{s_i,k} = 0$  **then**
  - 16:             remove  $s_i$  request in  $b_k$
  - 17:         **end if**
  - 18:     **end for**
  - 19: **end while**
  - 20: **end**
- 

### 6.3 Heuristic 3: Highest Minimum First (HMF)

With IMA, the slices are sorted in decreasing order based on the total required resources over the involving gNBs. As the key to reach the maximum TTR is the allocation of the minimum required sRBs on the same position over B for each slice, we propose then in HMF to sort the slices in decreasing order based on the minimum required resources over the gNBs set. Therefore, the minimum is computed at each iteration and the algorithm proceeds as follows:

- i ) Compute the minimum required tiles for all slices,  $s_i \in S^o$  over all B,  $M = (m_{s_i})_{s_i \in S}$ .

- ii ) sort the slices in decreasing order based on  $m_{s_i, s_i \in S}$  and generate the set  $S^o$  with ordered slices.
- iii ) allocate  $m_{s_i}$  sequentially with leaving the LCUS over each bin.
- iv ) update  $\gamma_{s_i, k}$  by subtracting  $m_{s_i}$ .
- v ) repeat the steps from **i** until **iv** for all  $s_i \in S^o$ . If  $\gamma_{s_i, k} = 0$ . Remove  $s_i$  from  $b_k$ .
- vi ) If  $\Gamma = 0$ , stop. Otherwise, repeat **v** until all the slices are assigned the required tiles over B.

---

**Algorithm 3** Heuristic3- HMF
 

---

```

1: Input: B, S,  $\Gamma$ 
2: Output: HMF sRBs allocation  $G^{IMA} = (g_k^{IMA})_{k \in B}$ 
3: set  $g_k^{HMF} = (\alpha_{k, f, t}^{s_i, \mu})_{f, t} = 0 \forall k \in B \quad \forall s_i \in S$ 
4: while  $\Gamma \neq 0$  do
5:   Compute  $M = (m_{s_i})_{s_i \in S^o}$ 
6:    $S^o \leftarrow$  sort S in decreasing order based on M
7:   for each gNB  $b_k \in B$  do
8:     for each slice  $s_i \in S^o$  do
9:       add  $m_{s_i}$  to the allocation with LCUS
10:      Update  $g_k^{IMA}$  by allocating  $m_{s_i}$  tiles subsequent sRBs
11:      remove the allocated objects from  $\gamma_{s_i, k}$ 
12:     end for
13:     Update  $\Gamma$  by removing the allocated  $m_{s_i}$  objects from  $\gamma_{s_i, k}$ 
14:     if  $\gamma_{s_i, k} = 0$  then
15:       remove  $s_i$  request in  $b_k$ 
16:     end if
17:   end for
18: end while
19: end

```

---

HMF and IMA are implemented with time complexity of  $O(n_b * \rho^2)$ .

## 6.4 TTR computation

Once the allocation is performed, an evaluation of the total amount of tied sRBs, the largest continuous unallocated space in a grid and convergence time is prominent. The LCUS and CT are computed as explained in section 5.1. With the ESRP model, the TTR was exactly the objective score. With the heuristics, the computation of TTR is required once the allocation finishes. For that, we propose an algorithm to count the total tied sRBs over the gNBs.

An sRB is considered as tied if it is allocated to same slice over the involved gNBs. In fact, each slice requests a different amount of resources on each gNB. The maximum tied sRBs between a given subset of gNBs is then equal to the minimum required resources over the same subset. An example includes, a slice  $s_1$  that requires 2 tiles (8 sRBs) on gNB  $b_1$  and 1 tile (4 sRBs) on gNB  $b_2$ . If

the allocation is optimal, we will have at maximum 1 tied tile for  $s_1$  over  $b_1$  and  $b_2$ , i.e. 4 tied sRBs.

From that, given the resource grid with complete allocation,  $G_c = g_k^c$ , we propose to count the total tied sRBs as summarized in algorithm 4 and explained in the following for each slices  $s_i \in S$ .

- i ) compute the total required sRBs for each slice,  $Max(s_i) = \sum_{k \in B} \gamma_{s_i, k}^\mu$ .
- ii ) select the gNBs where the slice requests the resources, noted  $B_{s_i}$
- iii ) compute the minimum required resources over  $B_{s_i}$ , i.e.  $Min(s_i) = \min_{k \in B_{s_i}} \gamma_{s_i, k}^\mu$ .
- iv ) compute the tied sRBs from  $Min(s_i)$  without redundancy.
- v ) update  $Max(s_i)$  and repeat from step 2.
- vi ) repeat from 2 until the total required sRBs is reached or there is no minimum sRBs between any gNBs to be tied.

---

**Algorithm 4** Total tied sRBs (TTR)

---

- 1: **Input:**  $G_c, S, B, \Gamma$ .
  - 2:
  - 3: **Output:** Total tied sRBs over  $B$ .
  - 4: **for each slice**  $s_i \in S$  **do**
  - 5:   Compute  $Max(s_i) = \sum_{k \in B} \gamma_{s_i, k}^\mu$
  - 6:   Compute the  $Min(s_i) = \min_{k \in B} \gamma_{s_i, k}^\mu$
  - 7:   **while**  $Max(s_i) \geq 0$  and  $Min(s_i) \neq 0$  **do**
  - 8:      $B_{s_i} \leftarrow \{b_k, k \in B \text{ where } \gamma_{s_i, k}^\mu \neq 0\}$
  - 9:      $Min(s_i) = \min_{k \in B_{s_i}} \gamma_{s_i, k}^\mu$
  - 10:     count  $\theta_j$  from  $Min(s_i)$  and check the non redundancy.
  - 11:     update  $Max(s_i) \leftarrow Max(s_i) - 4 * Min(s_i)$
  - 12:   **end while**
  - 13:    $\Theta_{s_i} = \sum_{j \in \zeta_{s_i}} \theta_j$
  - 14: **end for**
  - 15:  $\chi = \sum_{s_i \in S} \Theta_{s_i}$
- 

This algorithm is validated based on ESRP models. For all the instances of ESRP simulations, the achieved optimal TTR by ESRP is compared to the one computed by algorithm 4.

## 7 Heuristics Evaluation

In this section, the performance evaluation of the three heuristics is presented. It mainly deals with comparing the three heuristics based on CT, TTR and LCUS. For that, the heuristics achieved TTR is compared with the optimal/upper-bound TTR given by the ESRP model. Regarding the MCUS, although the skyline has reached the optimal LCUS for the different B and S sizes, the comparison between the three heuristics LCUS is performed with

respect to the topmost upper bound score (LTUB). Furthermore, for all evaluations, the impact of the gNBs number and the served slices is also investigated. The simulation environment and process is exactly as described in part 5.2. The results are then averaged over all the simulations runs for each test having a fixed size of slices and gNBs sets, and different slicing profile.

### 7.1 TTR Analysis

Fig. 16 illustrates the TTR optimality gap achieved by the 3 algorithms as a function of B size. The optimality gap (OG) is obtained from the difference between the optimal/upper bound score given by ESRP and the achieved score by a given algorithm divided by the optimal/upper score. It refers to the gap between the reached score and the optimal/upper-bound one. In order to have good insight on the OG values interpretation, Fig. 15 exhibits the total number of simulations run where the ESRP model converges at the time limit of 600 s, i.e. total number of reached optimal value by ESRP. As a reminder, for each B and S set size, 100 simulations run is performed and for each one the SPFM is tested before running ESRP and the heuristics. Hence, some infeasible slicing profiles are rejected in the SPFM level. Thus, as shown on Fig 8, ESRP has reached the optimal TTR for all the simulations run when the system is serving 3 slices and the gNBs set is varying from 2 to 5 gNBs. Therefore, the OG calculation for these sets combination is based on the optimal TTR score. Further, for the other B and S sets combinations, especially the larger ones, OG is counted using the upper-bound value given by the system. The upper-bound value is still idealistic, and might not be reached by the solver even when letting the simulation running over for days. In our analysis, we consider an OG as good if it is lower than 50%, acceptable between 50% and 80%, and poor for values exceeding 80%.

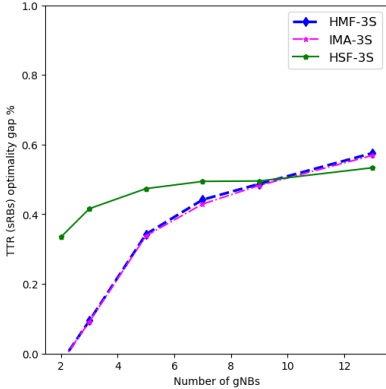
B size \ S size	2	3	5	7	9	13
3	87	61	55	58	51	45
5	63	35	14	9	11	13
7	38	14	2	1		
9	22	4				
11	14	2		1		
13	11	3				
15	3					

Fig. 15: ESRP optimal gap (OG) achievements. For each B and S size, the number of simulations runs reaching the optimal score before the time limit of 600 s is shown.



From Fig. 16, IMA and HMF have quite similar results over the various B set sizes, i.e. their curves colored in blue and purple respectively are superposing. They reach the optimality for lower B set sizes when serving different S sizes (see Fig. 16), i.e. OG=0%. The HSF is at 30% from optimality in similar cases. Then, the three heuristics scores increases proportionally to B size augmentation, but still lower than 50%. Both algorithms outperform HSF for B sizes lower than 9 gNBs.

As for the impact of S size on TTR, Fig. 17 shows the OG as a function of S for two system sizes: 3 and 5 gNBs. The OG increases when moving from a system serving 3 slices to the one with 7 slices. Then, the OG is quite stable around 22% with 3 gNBs and 47% with 5 gNBs with both IMA and HMF. It can be concluded that HMF and IMA become insensitive to larger S set size starting from 7 slices, while achieving a good OG. It is mainly the B set size that has an impact on the TTR score. The HSF has higher OG compared to HMF and IMA, but remains acceptable. Its OG score ranges between 47% and 74% with a system of 5 gNBs.



**Fig. 16:** TTR (sRBs) Optimality gap as a function of B size serving 3 slices.

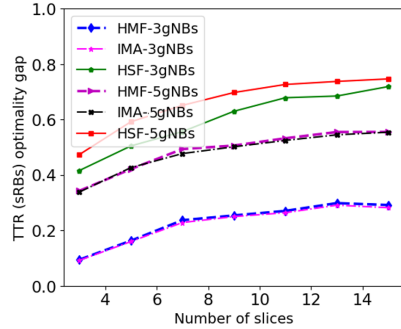


**Fig. 17:** TTR (sRBs) Optimality gap as a function of S for different B size.

Thus, IMA and HMF always outperform HSF in the case of 3 gNBs as well as 5 gNBs. Overall, the OG scores achieved by IMA and HMF are considered as good. Both heuristics reached the optimal scores given by ESRP for lower B and S set sizes. For the larger sets such as 13 gNBs and 15 slices, OG of IMA and HMF does not exceed 75%. Hence, an acceptable OG values are achieved. More importantly, unlike the ESRP objective to reach only the optimal TTR, the developed heuristics assure at best the TTR while guarantying the MCUS objective as well. In other words, the heuristics are ensuring the 5G cooperation enabling requirement with good OG while guarantying the three other requirements, i.e. scalability, satisfaction and orthogonality.

## 7.2 Convergence Time (CT) Analysis

Fig. 18 shows the convergence time of the three heuristics in seconds as function of  $B$  serving 3 slices. The three heuristics converge quickly at a time scale of hundreds of milliseconds. IMA and HMF have similar CT and slight difference is remarked with HSF. The CT increases proportionally with  $B$  size growth. It expands gradually in the order of milliseconds. The CT is less than 10 ms for small  $B$  set size. Regarding the  $S$  size impact on CT, Fig. 19 plots the three heuristics CT as a function of  $S$  size with a system of 3 gNBs. The three heuristics converge in similar time granularities and this is caused by using Skyline as an underlying algorithm for the heuristics. The CT varies in small interval size and it is independent of the  $S$  size. Notably, for a system with 3 gNBs, the IMA CT ranges between 0.04 s and 0.11 s.

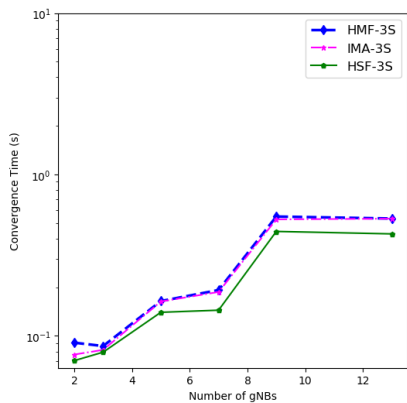


Fig. 18: CT (s) evaluation over varying  $B$  set size.

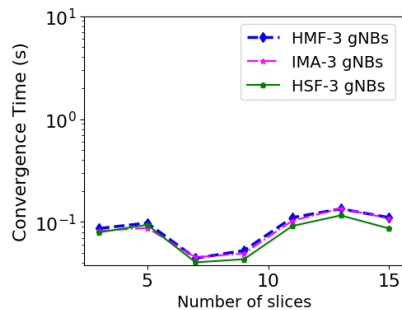
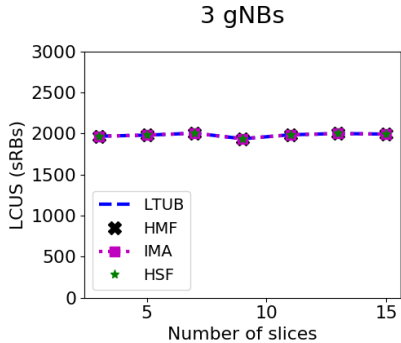


Fig. 19: CT (s) evaluation over varying  $S$  size.

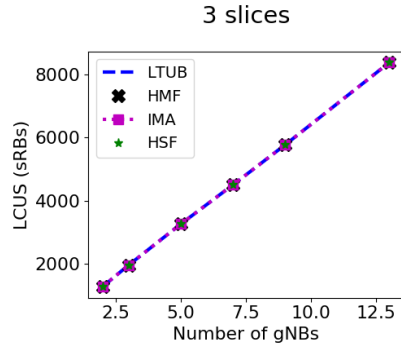
## 7.3 Maximization of the Continuous unallocated Space (MCUS) Analysis

Fig. 20 highlights the impact of  $S$  size on LCUS score in the system. The LCUS is computed over  $B$  as described in 5.1.3. Thus, we retrieve the number of free sRBs after the allocation is over. This free sRBs could be used by the SD-RAN controller to serve new accepted slices or increase the demand of an already served slices. Therefore, the 5G scalability requirement is evaluated in this section. The three heuristics achieve the optimal LCUS score given by LTUB. This is expected, as the skyline is used for the allocation. With  $S$  variation, the LCUS also varies in a small interval. This variation is independent of the  $S$  size evolution.

As for  $B$  size impact, Fig. 21 plots the LCUS over each  $B$  set size. All heuristics achieve the optimal LCUS score over the different  $B$  set sizes, i.e. their curves are superposing. It is observed that larger  $B$  sets allows higher gain in terms of LCUS by all approaches. The LCUS score is then proportional to the  $B$  set size and insensitive to  $S$  size variation.



**Fig. 20:** LCUS (sRBs) as a function of  $S$  for a system with 3 gNBs.



**Fig. 21:** LCUS (sRBs) as a function of  $B$  serving 3 slices.

## 7.4 Discussion

In order to enforce the real time RAN slicing, we proposed three heuristics, i.e. IMA, HMF and HSF that prioritize the LCUS while the TTR is achieved at best. An evaluation of the three heuristics is fulfilled based on CT, TTR and the LCUS. Contrarily to the ESRP model, the three heuristics converge at time scale of milliseconds. For lower  $B$  and  $S$  set sizes (i.e. less than 3 gNBs and 5 slices respectively) the CT is in the order of 10 ms. The CT increases smoothly with larger  $B$  set size. But, it does not outpace 0.7 s, 0.65 s, and 0.47s when tested with HMF, IMA and HSF respectively in a large  $B$  set of 13 gNBs serving 15 slices simultaneously. From that, these heuristics demonstrate their capability for real time deployment within the 5G SD-RAN.

Further, the HMF, HSF and IMA heuristics are compared to the optimal/upper bound solution given by ESRP for the TTR score. For the LCUS, the heuristics are compared with the upper bound LCUS (LTUB). For a small set of gNBs and slices, the IMA and HMF are highly enforcing the RAN slicing for real time system deployment by reaching the optimality for TTR and LCUS in very small time scales (in the order of 10 ms). This could be the case of macro cells deployment, as well as a small group of other cells type covering a specific geographical zone. Moreover, higher  $S$  size does not have a big impact on both IMA and HMF with respect to TTR, which is advantageous for the 5G RAN enforcement. Both heuristics performance degrade with larger  $B$  sets. But, in the worst case study of 13 gNBs serving 15 slices, at least 32% of the optimal TTR is reached by both heuristics. This score might be higher as the ESRP does not converge within the time limit for this instances, and then the comparison is conducted with the upper bound TTR. Nevertheless, this score is still advantageous as the heuristics prioritize the LCUS at the expense of TTR. In fact, the highest  $B$  size produce the highest LCUS when applying both heuristics. It corresponds exactly to the optimal LCUS marked by the LCUS upper bound. Thus, they lead to an allocation without resources

waste. This prioritization is intended because of the crucial task of efficient resource allocation required by the MNO.

In summary, although the ESRP model gives the optimal allocation with higher total tied sRBs, its high convergence time and non assurance of resources efficient usage make its real time deployment questionable. The IMA, HMF and HSF heuristics achieve good results in terms of TTR, CT and largest unallocated space for lower B sets. This proves the possibility of their real time deployment for such cases. The growth of B size allows a larger continuous unallocated space at the expense of TTR with all the developed heuristics. Even-though this priority prospect, the TTR is assured at best by HSF, IMA and HMF. The HMF and IMA are outperforming the HSF. Thus, the slice owner could use the tied resources to enable the advanced transmission schemes, e.g. IBSPC, CoMP, for the critical transmissions. Moreover, all heuristics highly enforce the RAN slicing with respect to the four requirements. In fact, the orthogonality, satisfaction and scalability are guaranteed, while the enabling requirement is assured at best.

## 8 Conclusion

The RAN slicing comes with challenging requirements such as resources isolation, slices satisfaction, scalability and the cooperation enabling. In this work, we aimed to enforce it from resource perspective in the 5G context. For that, we have formulated the problem as a multi-objective optimization to allocate efficiently the slices resources with respect to the diverse RAN slicing requirements. The first objective addresses the scalability of the RAN slicing through the maximization of the largest continuous unallocated space on each gNB resource grid. Then, the second objective handles the cooperation enabling requirements by means of resource allocation in similar position over frequency and time for a given slice over the set of gNBs. The second objective involves a tight management of resources. Therefore, a resource grid decomposition is proposed as to have a fine grained resources monitoring. Both slices resources isolation and satisfaction are guaranteed by means of constraint in each objective.

With the multi-objective criterion, the optimal solution for each objective is targeted. A mathematical model is developed for the first objective, whereas the second objective is tackled as a 2D bin packing optimization problem. An heuristic is then used to approximate rapidly the optimal score, as the problem is known to be NP-hard. The optimal models converge slowly, which limits their deployment for real time use cases. Nevertheless, they could be advantageous for the SD-RAN large scale decisions.

Therefore, three heuristics are implemented with the aim to enforce the allocation strategy for the RAN slicing. The scalability is prioritized with these heuristics at the expense of the enabling cooperation requirement. All the algorithms are evaluated in terms of convergence time, total tied resources and largest continuous unallocated space.

Contrarily to the mathematical model, the developed heuristics, i.e. IMA, HMF and HSF achieve good results in different case studies. Especially, for lower set of gNBs, the IMA and HMF reach the optimal scores for both tied resources with optimality gap of 0% and largest unallocated continuous space with a very low convergence time in the order of 10 ms. Such time is highly convenient for real time deployment, as it allows the controller to change the allocation at the frequency of the frame duration. Moreover, in such case the four RAN slicing requirements are guaranteed: orthogonality, satisfaction, scalability and cooperation enabling are assured by the heuristics. For real time deployment scenarios, the slices set size has an impact on the centralization benefit and the processing function migration [44]. In this work, all the tested algorithms show insensitivity to the number of served slices during the allocation window, even when it reaches 15 slices (i.e. maximum realistic slice set size). Therefore, this results encourage the real time deployment test for the three approaches.

In this work, we have been mainly interested in the allocation over a cluster of gNBs controlled by one SD-RAN. Our future work concerns the RAN slicing enforcement in multi-SD-RAN multi-cell deployment. In such case, a coordination or a cooperation between SD-RANs should be investigated for large resources allocation with respect to slicing requirements.

## References

- [1] Chahbar, M., Diaz, G., Dandoush, A., Cérin, C., Ghoumid, K.: A comprehensive survey on the e2e 5g network slicing model. *IEEE Transactions on Network and System Management (TNSM)* **18**(1), 49–62 (2021). <https://doi.org/10.1109/TNSM.2020.3044626>
- [2] Shen, X., Gao, J., Wu, W., Lyu, K., Li, M., Zhuang, W., Li, X., Rao, J.: Ai-assisted network-slicing based next-generation wireless networks. *IEEE Open Journal of Vehicular Technology (VTS)* **1** (2020)
- [3] Gil Herrera, J., Botero, J.F.: Resource allocation in nfv: A comprehensive survey. *IEEE Transactions on Network and Service Management* **13**(3), 518–532 (2016). <https://doi.org/10.1109/TNSM.2016.2598420>
- [4] Shin, M.-K., Nam, K.-H., Kim, H.-J.: Software-defined networking (sdn): A reference architecture and open apis. In: 2012 International Conference on ICT Convergence (ICTC), pp. 360–361 (2012). <https://doi.org/10.1109/ICTC.2012.6386859>
- [5] Qazi, Z.A., Walls, M., Panda, A., Sekar, V., Ratnasamy, S., Shenker, S.: A high performance packet core for next generation cellular networks. In: Proceedings of the Conference of the ACM Special Interest Group on Data Communication - SIGCOMM '17, pp. 348–361 (2017). <https://doi.org/10.1145/3098822.3098848>. Los Angeles, CA, USA.

<http://dl.acm.org/citation.cfm?doid=3098822.3098848>

- [6] Foukas, X., Marina, M.K., Kontovasilis, K.: Orion: Ran slicing for a flexible and cost-effective multi-service mobile network architecture. In: Proceedings of the 23rd Annual International Conference on Mobile Computing and Networking - MobiCom '17, pp. 127–140 (2017). <https://doi.org/10.1145/3117811.3117831>. Snowbird, Utah, USA. <http://dl.acm.org/citation.cfm?doid=3117811.3117831>
- [7] Coronado, E., Khan, S.N., Riggio, R.: 5g-empower: A software-defined networking platform for 5g radio access networks. *IEEE Transactions on Network and System Management (TNSM)* **16**(2), 715–728 (2019). <https://doi.org/10.1109/TNSM.2019.2908675>
- [8] Lee, D., Seo, H., Clerckx, B., Hardouin, E., Mazzaresse, D., Nagata, S., Sayana, K.: Coordinated multipoint transmission and reception in lte-advanced: Deployment scenarios and operational challenges. *IEEE Communications Magazine* **50**(2), 148–155 (2012). <https://doi.org/10.1109/MCOM.2012.6146494>
- [9] Elayoubi, S.E., Jemaa, S.B., Altman, Z., Galindo-Serrano, A.: 5g ran slicing for verticals: Enablers and challenges. *IEEE Communications Magazine* **57**(1), 28–34 (2019). <https://doi.org/10.1109/MCOM.2018.1701319>
- [10] D’Oro, S., Restuccia, F., Talamonti, A., Melodia, T.: The slice is served: Enforcing radio access network slicing in virtualized 5g systems. In: *IEEE INFOCOM 2019 - IEEE Conference on Computer Communications*, pp. 442–450 (2019). <https://doi.org/10.1109/INFOCOM.2019.8737481>. Paris, France. <https://ieeexplore.ieee.org/document/8737481/>
- [11] Devlic, A., Hamidian, A., Liang, D., Eriksson, M., Consoli, A., Lundstedt, J.: Nesmo: Network slicing management and orchestration framework. In: *2017 IEEE International Conference on Communications Workshops (ICC Workshops)*, pp. 1202–1208 (2017). <https://doi.org/10.1109/ICCW.2017.7962822>. Paris, France. <http://ieeexplore.ieee.org/document/7962822/>
- [12] Ferrus, R., Sallent, O., Perez-Romero, J., Agusti, R.: On 5g radio access network slicing: Radio interface protocol features and configuration. *IEEE Communications Magazine* **56**(5), 184–192 (2018). <https://doi.org/10.1109/MCOM.2017.1700268>
- [13] Koutlia, K., Ferrús, R., Coronado, E., Riggio, R., Casadevall, F., Umbert, A., Pérez-Romero, J.: Design and experimental validation of a software-defined radio access network testbed with slicing support. *Hindawi journal on Wireless Communications and Mobile Computing* **2019** (2019). <https://doi.org/10.1155/2019/2361352>

- [14] Marquez, C., Gramaglia, M., Fiore, M., Banchs, A., Costa-Pérez, X.: Resource sharing efficiency in network slicing. *IEEE Transactions on Network and Service Management* **16**(3), 909–923 (2019). <https://doi.org/10.1109/TNSM.2019.2923265>
- [15] Yan, M., Feng, G., Zhou, J., Sun, Y., Liang, Y.-C.: Intelligent resource scheduling for 5g radio access network slicing. *IEEE Transactions on Vehicular Technology* **68**(8), 7691–7703 (2019). <https://doi.org/10.1109/TVT.2019.2922668>
- [16] Mandelli, S., Andrews, M., Borst, S., Klein, S.: Satisfying network slicing constraints via 5g mac scheduling. In: *IEEE INFOCOM 2019 - IEEE Conference on Computer Communications*, pp. 2332–2340 (2019). <https://doi.org/10.1109/INFOCOM.2019.8737604>. Paris, France. <https://ieeexplore.ieee.org/document/8737604/>
- [17] B. Han, L.J., Schotten, H.D.: Slice as an evolutionary service: Genetic optimization for inter-slice resource management in 5g networks, *iee access*, vol. 6, no. 1. p **33**, 137 (2018)
- [18] Yang, X., Wang, Y., Wong, I.C., Liu, Y., Cuthbert, L.: Genetic algorithm in resource allocation of ran slicing with qos isolation and fairness. In: *IEEE Latin-American Conference on Communications (LATINCOM)* (2020). <https://doi.org/10.1109/LATINCOM50620.2020.9282290>
- [19] Chang, C.-Y., Nikaein, N., Spyropoulos, T.: Radio access network resource slicing for flexible service execution. In: " in *IEEE INFOCOM 2018-IEEE Conference on Computer Communications Workshops (INFOCOM WKSHPS)*. IEEE pp. 668–673, ??? (2018)
- [20] Papa, A., Klugel, M., Goratti, L., Rasheed, T., Kellerer, W.: Optimizing dynamic ran slicing in programmable 5g networks. In: *IEEE International Conference on Communications (ICC)*, pp. 1–7 (2019). <https://doi.org/10.1109/ICC.2019.8761163>. Shanghai, China
- [21] Ojaghi, B., Adelantado, F., Antonopoulos, A., Verikoukis, C.: Slicedran: Service-aware network slicing framework for 5g radio access networks. In: *IEEE Systems Journal* (2021). <https://doi.org/10.1109/JSYST.2021.3064398>
- [22] Hossain, A., Ansari, N.: 5g multi-band numerology-based tdd ran slicing for throughput and latency sensitive services. *IEEE Transactions on Mobile Computing* (2021). <https://doi.org/10.1109/TMC.2021.3106323>
- [23] Zambianco, M., Verticale, G.: Spectrum allocation for network slices with inter- numerology interference using deep reinforcement learning. In: *IEEE 31st Annual International Symposium on Personal, Indoor and*

- Mobile Radio Communications, pp. 1–7 (2020). <https://doi.org/10.1109/PIMRC48278.2020.9217107>
- [24] Khodapanah, B., Awada, A., Viering, I., Barreto, A.N., Simsek, M., Fettweis, G.: Slice management in radio access network via deep reinforcement learning. IEEE 91st Vehicular Technology Conference (VTC2020-Spring), 1–6 (2020). <https://doi.org/10.1109/VTC2020-Spring48590.2020.9128982>
- [25] Raftopoulou, M., Litjens, R.: Optimisation of numerology and packet scheduling in 5g networks: To slice or not to slice? IEEE 93rd Vehicular Technology Conference (VTC2021- Spring), 1–7 (2021). <https://doi.org/10.1109/VTC2021-Spring51267.2021.9448814>
- [26] Korrai, P.K., Lagunas, E., Bandi, A., Sharma, S.K., Chatzinotas, S.: Joint power and resource block allocation for mixed-numerology-based 5g downlink under imperfect csi. IEEE Open Journal of the Communications Society **1**, 1583–1601 (2020). <https://doi.org/10.1109/OJCOMS.2020.3029553>
- [27] Alves Esteves, J.J., Boubendir, A., Guillemin, F., Sens, P.: Heuristic for edge-enabled network slicing optimization using the “power of two choices”. 16th International Conference on Network and Service Management (CNSM), 1–9 (2020). <https://doi.org/10.23919/CNSM50824.2020.9269099>
- [28] Wang, G., Feng, G., Quek, T.Q.S., Qin, S., Wen, R., Tan, W.: Reconfiguration in network slicing —optimizing the profit and performance. IEEE Transactions on Network and Service Management **16**(2), 591–605 (2019). <https://doi.org/10.1109/TNSM.2019.2899609>
- [29] Harutyunyan, D., Fedrizzi, R., Shahriar, N., Boutaba, R., Riggio, R.: Orchestrating end-to-end slices in 5g networks. In: 15th International Conference on Network and Service Management (CNSM), pp. 1–9 (2019). <https://doi.org/10.23919/CNSM46954.2019.9012732>. Halifax, Canada
- [30] Mahindra, R., Khojastepour, M.A., Zhang, H., Rangarajan, S.: Access network sharing in celluradio access network sharing in cellular networks. In: 2013 21st IEEE International Conference on Network Protocols (ICNP), pp. 1–10 (2013). <https://doi.org/10.1109/ICNP.2013.6733595>
- [31] He, J., Song, W.: Appran: Application-oriented radio access network sharing in mobile networks. In: 2015 IEEE International Conference on Communications (ICC), pp. 3788–3794 (2015). <https://doi.org/10.1109/ICC.2015.7248914>. London, UK. <http://ieeexplore.ieee.org/document/7248914/>



- [32] Sallent, O., Perez-Romero, J., Ferrus, R., Agusti, R.: On radio access network slicing from a radio resource management perspective. *IEEE Wireless Communications* **24**(5), 166–174 (2017). <https://doi.org/10.1109/MWC.2017.1600220WC>
- [33] Zambianco, M., Verticale, G.: Interference minimization in 5g physical-layer network slicing. *IEEE Transactions on Communications* **68**(7), 4554–4564 (2020). <https://doi.org/10.1109/TCOMM.2020.2983009>
- [34] Mei, J., Wang, X., Zheng, K.: An intelligent self-sustained ran slicing framework for diverse service provisioning in 5g-beyond and 6g networks. *Intelligent and Converged Networks* **1**(3), 281–294 (2020). <https://doi.org/10.23919/ICN.2020.0019>
- [35] Sciancalepore, V., Samdanis, K., Costa-Perez, X., Bega, D., Gramaglia, M., Banchs, A.: Mobile traffic forecasting for maximizing 5g network slicing resource utilization. In: *IEEE INFOCOM 2017 - IEEE Conference on Computer Communications*, pp. 1–9 (2017). <https://doi.org/10.1109/INFOCOM.2017.8057230>. Atlanta, GA, USA. <http://ieeexplore.ieee.org/document/8057230/>
- [36] Perez-Romero, J., Vila, I., Sallent, O., Blanco, B., Sanchoyerto, A., Solozabal, F., Liberal, F.: Supporting mission critical services through radio access network slicing. In: *International Conference on Information and Communication Technologies for Disaster Management (ICT-DM)*, pp. 1–8 (2019). <https://doi.org/10.1109/ICT-DM47966.2019.9032966>
- [37] Gebremariam, A.A., Chowdhury, M., Usman, M., Goldsmith, A., Granelli, F.: Softslice: Policy-based dynamic spectrum slicing in 5g cellular networks. In: *2018 IEEE International Conference on Communications (ICC)*, pp. 1–6. IEEE, ??? (2018). <https://doi.org/10.1109/ICC.2018.8422148>. Kansas City, MO, USA. <https://ieeexplore.ieee.org/document/8422148/>
- [38] Caballero, P., Banchs, A., de Veciana, G., Costa-Perez, X.: Network slicing games: Enabling customization in multi-tenant networks. In: *IEEE INFOCOM 2017 - IEEE Conference on Computer Communications*, pp. 1–9 (2017). <https://doi.org/10.1109/INFOCOM.2017.8057046>. Atlanta, GA, USA. <http://ieeexplore.ieee.org/document/8057046/>
- [39] Jia, Y., Tian, H., Fan, S., Zhao, P., Zhao, K.: Bankruptcy game based resource allocation algorithm for 5g cloud-ran slicing. In: *2018 IEEE Wireless Communications and Networking Conference (WCNC)*, pp. 1–6 (2018). <https://doi.org/10.1109/WCNC.2018.8377187>. Barcelona, Spain. <https://ieeexplore.ieee.org/document/8377187/>
- [40] Wallace, M.: ractical applications of constraint programming. *Constraints*

- 1(1–2), 139–168 (1996). <https://doi.org/10.1007/BF00143881>
- [41] Garey, M.R., Johnson, D.S.: *Computers and Intractability: a Guide to The Theory of NP-Completeness*, 27. print edn. A series of books in the mathematical sciences, (2009)
- [42] Jylänki, J.: *A Thousand Ways to Pack the Bin – a Practical Approach to Two-Dimensional Rectangle Bin Packing* (2010)
- [43] He, L., Ren, X., Gao, Q., Zhao, X., Yao, B., Chao, Y.: The connected-component labeling problem: A review of state-of-the-art algorithms. *Pattern Recognition* **70**, 25–43 (2017). <https://doi.org/10.1016/j.patcog.2017.04.018>
- [44] Sen, N., Franklin, A.A.: Impact of slice granularity in centralization benefit of 5g radio access network. In: *2020 6th IEEE Conference on Network Softwarization (NetSoft)*, pp. 15–21 (2020). <https://doi.org/10.1109/NetSoft48620.2020.9165366>

## 9 Authors' biographies

**Imane Oussakel** received a PhD in 2020 from Paul Sabatier University, Toulouse III. His main interests deal with new generation cellular networks. She is currently working as the 5G project manager for the French Orange network operator on the development and deployment of new 5G facilities.

**Philippe Owezarski** is director of research at CNRS (the French center for scientific research), working at LAAS (Laboratory for Analysis and Architecture of Systems), in Toulouse, France. He got a PhD in computer science in 1996 from Paul Sabatier University, Toulouse III, and habilitation for advising research in 2006. His main interests deal with networks of the future. More specifically Philippe Owezarski takes advantage of IP networks monitoring for enforcing Quality of Service and security. It especially focuses on techniques as machine learning and data mining on the big data collected from the networks for making the network related analytics autonomous and cognitive.

**Pascal Berthou** received a Ph.D. in computer science and telecommunication from national polytechnic institute of Toulouse in 2001. He is associate professor at the Toulouse University of Science and member of the Laboratory for Analysis and Architecture of Systems of the French National Center for Scientific Research (LAAS/CNRS) since 1998. His main research interests deal with high-speed networks and protocols and multimedia communications. He especially works on satellite communication systems and sensors networks.

**Laurent Houssin** received the Ph.D. degree in automatic control and computer science from the University of Angers, France, in 2006. From 2007 to

2021, he has been associate professor at University of Toulouse, France. Since 2021, he has been associate professor at ISAE-Supaero, Toulouse, France. His current research interests include operations research and optimization.